RESEARCH ARTICLE

Retrograde transport is not required for cytosolic translocation of the B-subunit of Shiga toxin

Maria Daniela Garcia-Castillo[1,2,3], Thi Tran[4,5], Alexandre Bobard[6], Henri-François Renard[1,2,3], Stefan J. Rathjen[1,2,3], Estelle Dransart[1,2,3], Bahne Stechmann[1,2,3], Christophe Lamaze[2,3,7], Mike Lord[8], Jean-Christophe Cintrat[9], Jost Enninga[6], Eric Tartour[4,5] and Ludger Johannes[1,2,3,*]

ABSTRACT

Antigen-presenting cells have the remarkable capacity to transfer exogenous antigens to the cytosol for processing by proteasomes and subsequent presentation on major histocompatibility complex class-I (MHC-I) molecules, a process termed cross-presentation. This is the target of biomedical approaches that aim to trigger a therapeutic immune response. The receptor-binding B-subunit of Shiga toxin (STxB) has been developed as an antigen delivery tool for such immunotherapy applications. In this study, we have analyzed pathways and trafficking factors that are involved in this process. A covalent conjugate between STxB and saporin was generated to quantitatively sample the membrane translocation step to the cytosol in differentiated monocyte-derived THP-1 cells. We have found that retrograde trafficking to the Golgi complex was not required for STxB–saporin translocation to the cytosol or for STxB-dependent antigen cross-presentation. Depletion of endosomal Rab7 inhibited, and lowering membrane cholesterol levels favored STxB–saporin translocation. Interestingly, experiments with reducible and non-reducible linker-arm–STxB conjugates led to the conclusion that after translocation, STxB remains associated with the cytosolic membrane leaflet. In summary, we report new facets of the endosomal escape process bearing relevance to antigen cross-presentation.

KEY WORDS: Shiga toxin, Rab6, Rab5, Rab7, Sec22B, Lactamase, Endoplasmic reticulum, Golgi, Endosome, Retro compound, PPMP, Brefeldin-A, Bafilomycin A1, Methyl-beta-cyclodextrin, Cholesterol, Nanodomain, Microdomain, Raft, Cytotoxic T-lymphocyte, Dendritic cell, Antigen cross-presentation, Endosomal escape, Immunotherapy, Cancer, Infectious disease

INTRODUCTION

Bacterial and plant toxins rely on intracellular transport to reach their molecular targets in the cytosol and, thus, their study has yielded important information regarding the various trafficking pathways to intracellular locations (Smith et al., 2002). Membrane translocation from the endosome has been documented, as in the case of diptheria toxin, where acidification is used to drive the transfer of its catalytic subunit across endosomal membranes. By contrast, some toxins are shuttled by vesicular transport from endosomes to the Golgi complex and continue to the endoplasmic reticulum (ER) to enter the cytosol.

Shiga toxin (STx) and Shiga-like toxins (STx-1 and STx-2) are in this latter category. These are type II ribosome-inactivating proteins (RIPs) produced by *Shigella dysenteriae* and enterohemorrhagic strains of *Escherichia coli*, repectively (STx-1 is 99% identical in amino acid sequence to Shiga toxin). After binding to its cellular receptor, the Gb3 glycosphingolipid, the non-toxic B-subunit of Shiga toxin (STxB) transports the non-covalently linked catalytic A-subunit (STxA) along the retrograde route, via early endosomes, the trans-Golgi network (TGN) and Golgi cisternae, to the ER, from where STxA dislocates to the cytosol by exploiting the host ER-associated degradation (ERAD) machinery (Mallard et al., 1998; Spooner and Lord, 2012). STxA has N-glycosidase activity and inhibits protein biosynthesis by removing a specific adenine base from 28S rRNA of the 60S large ribosomal subunit.

STx is the causative agent for hemolytic uremic syndrome (Tarr et al., 2005). To date, no effective treatment or preventative measures exist against STx, and much effort has been aimed at finding specific inhibitors of these toxins. We previously identified two small molecule compounds, termed Retro-1 and Retro-2, which selectively blocked STx, ricin and cholera toxin retrograde transport at the early-endosome–TGN interface (Stechmann et al., 2010). Analysis of Retro-treated cells revealed that these compounds were selective, in that compartment morphology was preserved, and that no inhibition of retrograde transport of endogenous proteins, or of any other trafficking steps was observed. Importantly, Retro-2 protected mice against a lethal exposure to ricin.

Stimulation of CD8+ cytotoxic T-lymphocytes (CTLs) by antigen-presenting cells is a crucial component of protective and therapeutic immune responses against tumors and infectious diseases. It is now well established that dendritic cells possess the capacity to capture, process and present exogenous antigens to CTLs on major histocompatibility complex class-I (MHC-I) molecules; a process referred to as antigen cross-presentation. In the 'cytosolic pathway', antigens are translocated across internal membranes to access the cytosol where they are processed by proteaosomes and subsequently loaded by TAP transporters onto MHC-I molecules in the ER, or possibly in endocytic compartments (Kasturi and Pulendran, 2008). Some studies have shown that in dendritic cells, exogenous soluble antigens are delivered to the ER and retrotranslocated by molecular components required for ERAD, including the Sec61 channel and p97 (also known as VCP) (Ackerman et al., 2006, 2005; Wagner et al., 2012). Other studies demonstrated that purified phagosomes contain ER-associated molecules (calnexin, calreticulin), and therefore it has been

[1]Institut Curie, PSL Research University, Endocytic Trafficking and Therapeutic Delivery Group, 26 rue d'Ulm, Paris Cedex 05 75248, France. [2]CNRS UMR3666, Paris 75005, France. [3]INSERM U1143, Paris 75005, France. [4]INSERM U970, PARCC Université Paris Descartes Sorbonne Paris Cité, Paris 75006, France. [5]Hôpital Européen Georges-Pompidou, AP-HP, Service d'Immunologie Biologique, Paris Cedex 15 75908, France. [6]Dynamique des Interactions Hôte Pathogène, Institut Pasteur, Paris Cedex 15 75724, France. [7]Institut Curie – Centre de Recherche, Membrane Dynamics and Mechanics of Intracellular Signaling Group, 26 rue d'Ulm, Paris Cedex 05 75248, France. [8]Department of Biological Sciences, University of Warwick, Coventry CV4 7AL, UK. [9]CEA, iBiTec-S/SCBM, CEA-Saclay, LabEx LERMIT, Gif-sur-Yvette F-91191, France.

*Author for correspondence (ludger.johannes@curie.fr)

suggested that an autonomous cross-presentation compartment is created as the result of phagosomal fusion with the ER (now called the ER–phagosome fusion model) (Guermonprez et al., 2003). Consistent with this finding, it has been shown that the recruitment of ER-resident proteins to phagosomes, through the ER SNARE molecule Sec22B, is required for cross-presentation (Cebrian et al., 2011). Besides a requirement for ERAD machinery, another often-cited possibility for cytosolic export is the passage across endosomal membranes, as has been described for ricin and *Pseudomonas* exotoxin A (Beaumelle et al., 1993).

Some studies have provided direct evidence for an early endosomal contribution to cross-presentation of soluble antigens. Burgdorf and collegues have demonstrated that the mannose receptor specifically delivered the model antigen ovalbumin (OVA) into early endosomes leading to cross-presentation (Burgdorf et al., 2007), and that early endosomal soluble antigens recruited TAP for peptide loading (Burgdorf et al., 2008).

The Gb3 glycosphingolipid is expressed on human and mouse dendritic cells (Falguieres et al., 2001). Antigens fused or chemically coupled to the natural Gb3 ligand STxB, are targeted to dendritic cells, and delivered by receptor-dependent endocytosis, in a proteasome- and TAP-dependent manner, into the conventional MHC-I pathway, indicating that STxB-vectorized antigens are translocated to and processed in the cytosol (Haicheur et al., 2000; Lee et al., 1998). In mice, targeted delivery of exogenous peptides by STxB induces specific CTLs resulting in a potent and long-lasting immune response, and protection against tumor growth (Badoual et al., 2013; Haicheur et al., 2003; Pere et al., 2011; Sandoval et al., 2013; Vingert et al., 2006). The mechanisms leading to efficient antigen cross-presentation by STxB through the cytosolic pathway are not understood, and the trafficking factors that are involved in targeting STxB–antigen conjugates to membrane translocation competent compartments also remain to be identified.

Here, STxB–saporin and STxB–β-lactamase conjugates were developed to measure membrane translocation to the cytosol. We found that STxB–saporin-mediated inhibition of ribosomal activity in the cytosol was independent of retrograde transport to the Golgi, indicating that the translocation-competent organelle is an endosomal compartment. We identify endosomal trafficking factors and cholesterol as key modulators of STxB conjugate translocation to the cytosol, and provide evidence for a continued association of STxB with the cytosolic membrane leaflet once the protein has become exposed to the cytosolic milieu.

RESULTS
STxB–saporin conjugates in intoxication assays
To generate a quantitative, robust and scalable assay system for the study of mechanisms by which STxB conjugates translocate to the cytosol, STxB was covalently coupled to a cytotoxic moiety, the plant toxin saporin (Fig. 1A). Saporin must reach its cytosolic target, ribosomes, in order to inhibit protein biosynthesis. Cellular intoxication can therefore be used as a measure of the toxins' intracellular progression. Saporin is a type I RIP consisting of a single catalytically active chain with N-glycosidase activity (de Virgilio et al., 2010; Santanché et al., 1997). Cleavable (STxB–ss–saporin) and non-cleavable (STxB–saporin) conjugates were obtained (Advanced Targeting Systems, San Diego, CA) using previously described procedures (Polito et al., 2011). The purity of these conjugates was analyzed by SDS-PAGE on Tris-tricine gels (supplementary material Fig. S1A). To verify whether conjugation affected the ability of saporin to inactivate the ribosome, an *in vitro*

N-glycosidase activity assay was performed, as previously described (Smith et al., 2003). For both conjugates, the 360-base-pair 'aniline' fragment was generated as efficiently as with unconjugated saporin (supplementary material Fig. S1B,C), demonstrating that saporin activity was not altered by the conjugation process.

The use of saporin instead of antigenic peptides for coupling to STxB enabled us to use a cell intoxication assay to evaluate access to the cytosol, which is much simpler than measuring antigen cross-presentation. For this, cells were challenged with increasing doses of STx-1, STxB–saporin conjugates or unconjugated saporin, and protein biosynthesis was measured by monitoring the incorporation of radiolabeled methionine. Cytosolic arrival of a few catalytic chain molecules is enough to start inhibiting ribosomal activity, making this an exquisitely sensitive assay (Tam and Lingwood, 2007).

The monocytic cell line THP-1 and HeLa cells were chosen for our study. THP-1 cells express Gb3, are sensitive to STx (retrograde transport) (Ramegowda and Tesh, 1996) and can cross-present exogenous antigens (Gentschev et al., 2000). The 50% effective toxin concentration (EC_{50}) values were determined from dose–response intoxication curves, as described in the Materials and Methods. Analysis of EC_{50} values demonstrated that the covalent, but cleavable STxB–ss–saporin conjugate (the non-cleavable STxB–saporin conjugate will be presented later) required both a longer time and higher doses for intoxication as compared to STx-1 (non-covalent linkage between STxB and STxA) (Table 1). Dose-dependent intoxication by STx-1 was readily observed after a 1-h toxin challenge in both HeLa and THP-1 cells. By contrast, robust, dose-dependent protein biosynthesis inhibition by STxB–ss–saporin was seen only after a 4-h toxin exposure, suggesting its cytosolic target was reached through a different mechanism.

Both cell types also differed in their sensitivity to the saporin conjugate at later time points. Whereas no difference was observed between HeLa and THP-1 cells after a 24-h exposure to STx-1 holotoxin (Table 1; Fig. 1B), comparison of mean EC_{50} values showed that THP-1 cells were ~18.3-fold more sensitive than HeLa cells to the cleavable covalent STxB–ss–saporin conjugate (Table 1; Fig. 1C), suggesting that the mechanism for cytosolic access was not unique to antigen-presenting cells, but rather was more efficient in these cells.

We tested whether Gb3 was necessary for cell intoxication by STxB–ss–saporin. HeLa cells were cultured for 6 days in the presence of 5 μM D,L-threo-1-phenyl-2-palmitoylamino-3-morpholino-1-propanol (PPMP), inhibiting glycosphingolipid synthesis. In these PPMP-treated cells, STx-1 was no longer able to mediate protein biosynthesis inhibition, as expected (Fig. 1D). This was also the case for STxB–ss–saporin (Fig. 1E), providing evidence that cytosolic targeting of STxB–ss–saporin required binding to its glycosphingolipid receptor. In addition, unconjugated saporin was toxic only at the highest concentrations, where fluid-phase uptake becomes efficient (Fig. 1F), further demonstrating that STxB–ss–saporin-mediated protein synthesis inhibition was receptor-dependent.

Internalization and retrograde trafficking of STxB–saporin conjugates
STxB enters cells by clathrin-independent endocytosis (reviewed in Johannes et al., 2015) in a process that is operated in tight association with the BAR domain protein endophilin-A2 (endoA2, also known as SH3GL1) (Renard et al., 2015), which also functions
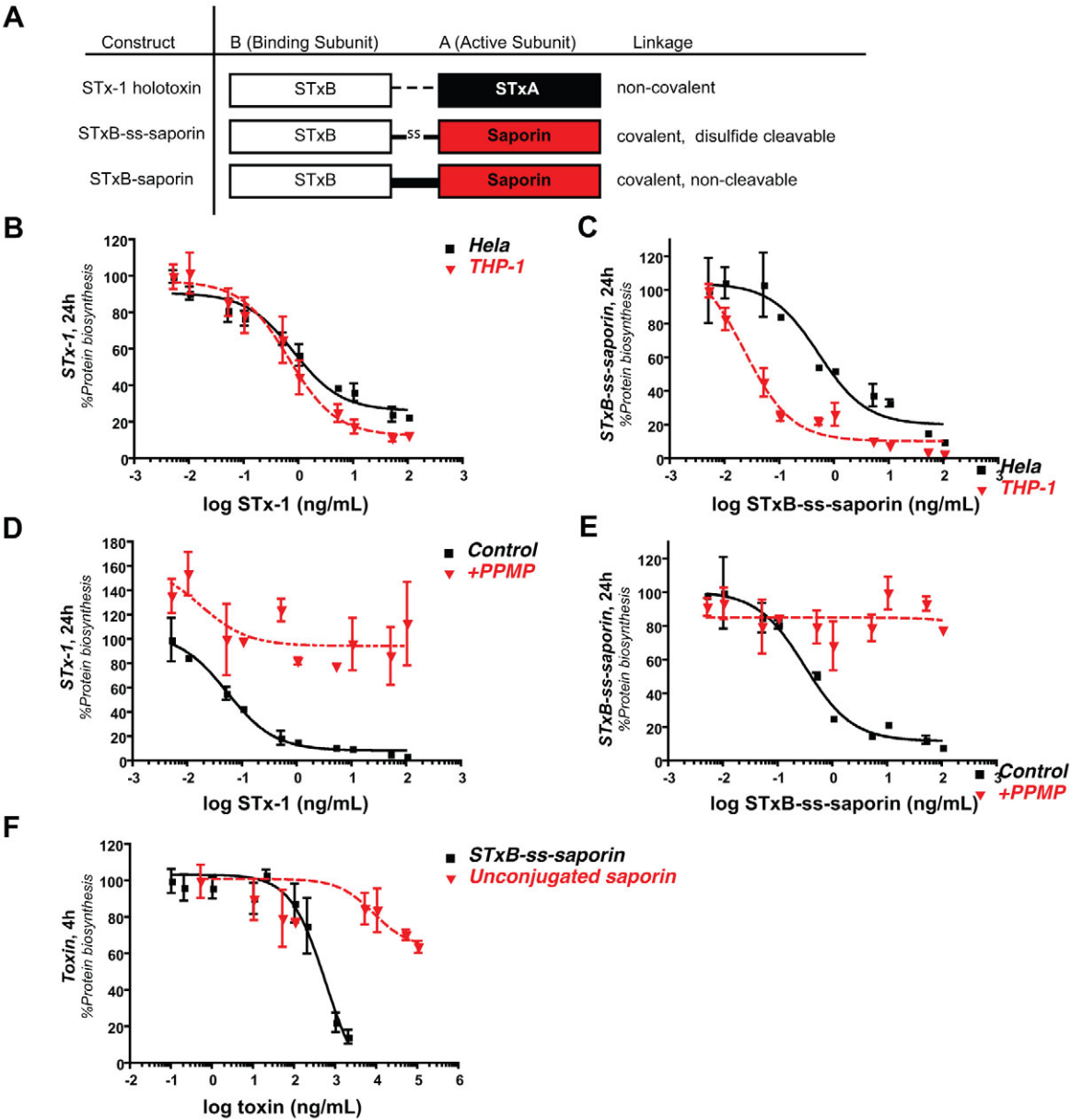
Fig. 1. Characterization of STxB-saporin conjugates. (A) Schematic representation of STxB–saporin conjugates. Covalent STxB–saporin conjugates were obtained by replacing STxA (black) with saporin (red) that was attached by a disulfide-cleavable or a non-cleavable linker arm. (B,C) Representative intoxication curves after a 24-h incubation of STx-1 or STxB–ss–saporin with HeLa (black curves) or THP-1 (red curves) cells. (D,E) HeLa cells were cultured for 6 days in the absence or presence of PPMP. After a 24 h exposure to (D) STx-1 or (E) STxB–ss–saporin protein synthesis was determined. (F) Intoxication assay comparing protein biosynthesis in HeLa cells incubated with STxB–ss–saporin or unconjugated saporin. Results are mean±s.e.m. of representative experiments in duplicate. See Table 1 for numbers of independent experiments.

in the clathrin-independent uptake processes of endogenous cellular proteins (Boucrot et al., 2015). In HeLa cells that stably expressed an endoA2–GFP fusion protein, we observed that STxB–ss–saporin colocalized as efficiently as STxB with endoA2 at the plasma membrane and in very early uptake intermediates (supplementary material Fig. S2A), strongly suggesting that its uptake pathway was not altered by conjugation to saporin. This conclusion was strengthened by the finding that STxB–ss–saporin and STxB

Table 1. HeLa or THP-1 cell intoxication by STx-1 or STxB–ss–saporin

EC$_{50}$ (ng/ml)	STx-1		STxB–ss–saporin	
	HeLa	THP-1	HeLa	THP-1
1 h	8.44±1.44 (n=12)	8.95±1.48 (n=10)	Does not converge (n=6)	Does not converge (n=6)
4 h	0.38±0.19 (n=12)	0.11±0.03 (n=16)	74.42±13.08 (n=10)	73.18±15.66 (n=10)
24 h	0.38±0.14 (n=6)	0.17±0.13 (n=12)	0.55±0.17 (n=8)	0.03±0.01 (n=10)

Mean EC$_{50}$ values were calculated after a 1, 4 and 24 h incubation with toxins from the indicated numbers of replicates for three to eight independent experiments. Data are mean±s.e.m.

strongly colocalized when co-incubated with HeLa cells for 5 min (supplementary material Fig. S2B).

STxB–ss–saporin was also efficiently transported to the Golgi complex after a 45-min incubation with HeLa cells at 37°C, as judged by the colabeling of anti-STxB antibodies with the Golgi marker giantin (also known as GOLGB1) (supplementary material Fig. S2C), and the colabeling of anti-STxB antibodies with anti-saporin antibodies in the perinuclear Golgi region (supplementary material Fig. S2D). In this, the STxB–ss–saporin conjugate ressembled wild-type STxB (see Mallard et al., 1998, and below). Importantly, the highly selective small-molecule inhibitor of early-endosome-to-TGN trafficking Retro-2 (Stechmann et al., 2010), caused the accumulation of STxB–ss–saporin in peripheral punctate structures (supplementary material Fig. S2C,D), confirming the trafficking of the protein through the retrograde route.

Having validated the Retro-2-dependent retrograde trafficking potential of STxB–ss–saporin in HeLa cells, we next analyzed whether this property was also conserved in THP-1 cells. To test

the Retro-2 compound, we first used standard conditions with Cy3-labeled wild-type STxB, as described previously (Stechmann et al., 2010). THP-1 cells were incubated on ice with Cy3–STxB, either in control conditions (0.05% DMSO) or after having been pre-treated at 37°C with 25 µM Retro-2. After washing, the cells were shifted for 45 min to 37°C, fixed, and antibody labeled. STxB (red) could be detected in the Golgi in control cells, as shown by its strong colocalization with the Golgi marker giantin (green) (Fig. 2A). In Retro-2-treated THP-1 cells, STxB was mostly localized in dispersed vesicular structures (Fig. 2B), indicating that in THP-1 cells, STxB transport to the TGN was also inhibited by Retro-2.

This conclusion was confirmed in a biochemical assay using the STxB variant STxB–Sulf$_2$, to which tandem sulfation sites have been added (Amessou et al., 2006; Mallard and Johannes, 2003). Briefly, when transported to the TGN, STxB–Sulf$_2$ becomes the substrate for active TGN-localized sulfotransferase, which catalyzes the specific transfer of radioactive sulfur from the medium onto a
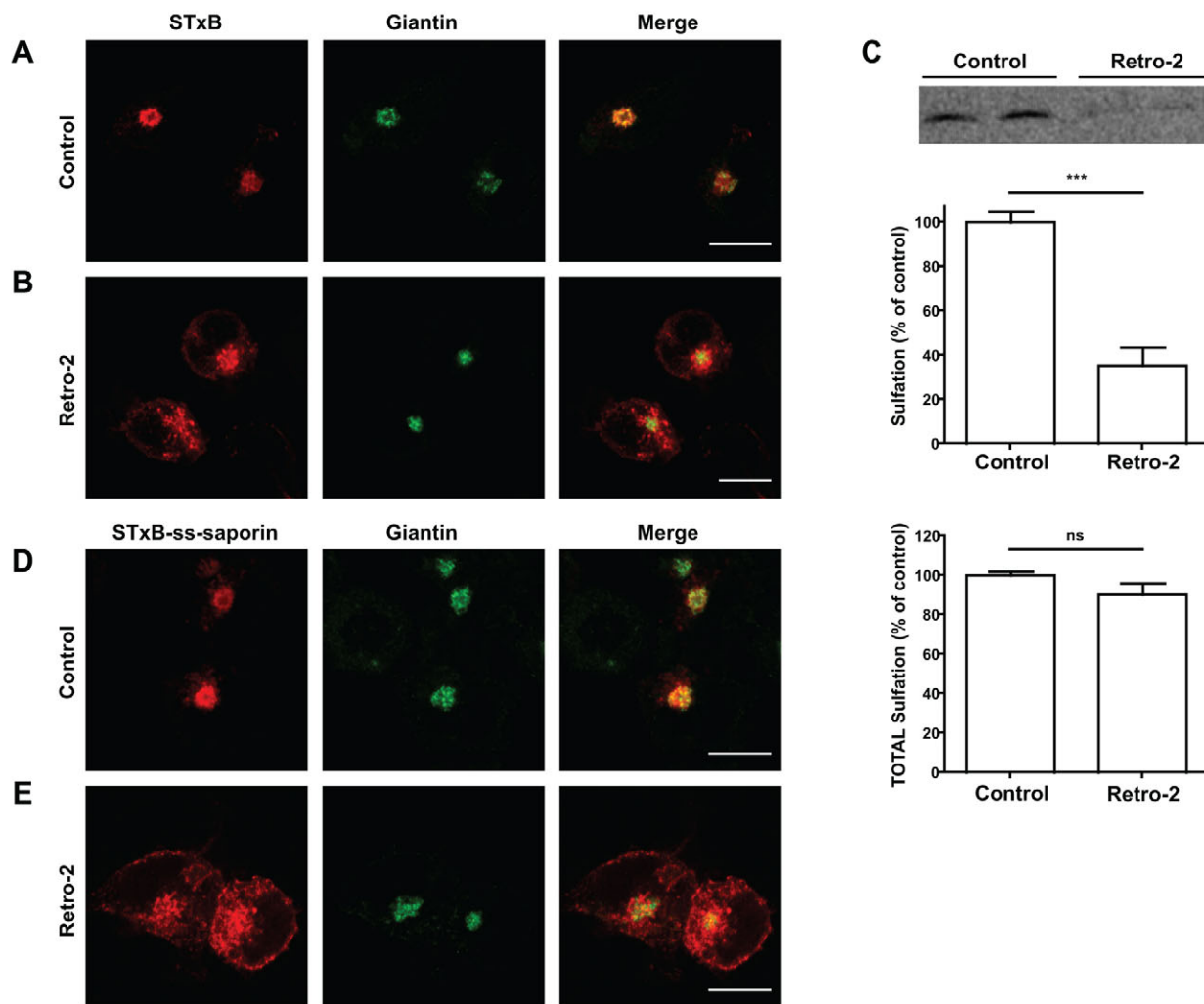

Fig. 2. Inhibition of retrograde STxB–ss–saporin transport by Retro-2 in THP-1 cells. (A,B) THP-1 cells were incubated with 0.5 µg/ml of Cy3-labeled STxB (red) after treatment with (A) DMSO or (B) 25 µM Retro-2. Cells were fixed and labeled with anti-giantin (green) antibody. Confocal images and a merge of both channels are presented. (C) Sulfation assay. 1 µM STxB–Sulf$_2$ was incubated on ice with THP-1 cells in control (0.05% DMSO) conditions or after treatment with 25 µM Retro-2. After incubation for 30 min at 37°C, sulfated STxB–Sulf$_2$ was detected by autoradiography. The autoradiogram is of a representative experiment. Results represent means±s.e.m. (n=4; two independent experiments). ***P<0.001, ns, not significant (unpaired one-tailed Student's t-test). (D,E) THP-1 cells were incubated with 0.5 µg/ml STxB–ss–saporin after treatment with (D) 0.05% DMSO or (E) 25 µM Retro-2, fixed and immunolabeled with anti-STxB (red) and anti-giantin (green) antibodies. Scale bars: 10 µm.

tyrosine residue within the sulfation sequence. Detection of sulfated STxB–Sulf$_2$ by autoradiography then serves as a quantitative measure of STxB arrival to the TGN. In Retro-2-treated THP-1 cells, we observed a 64.69%±9.48 (mean±s.e.m., n=4, two independent experiments) loss of sulfation signal, as compared to DMSO-treated control THP-1 cells (Fig. 2C), values which are in agreement with our previous results on HeLa cells (Stechmann et al., 2010) and are indicative of efficient retrograde transport inhibition. Moreover, total sulfation levels were not affected under Retro-2 treatment, providing evidence that THP-1 cells were in a healthy state and that the inhibitory effect was not due to altered sulfotransferase activity (Fig. 2C).

Next, we examined the intracellular trafficking of the STxB–ss–saporin conjugate in THP-1 cells through immunofluorescence experiments, as described above for HeLa cells. In control conditions, STxB–ss–saporin (red) strongly colocalized with giantin (green; Fig. 2D), indicating that the conjugate was also transported to the Golgi in THP-1 cells. In the presence of Retro-2, STxB–ss–saporin appeared to be in dispersed vesicular structures (Fig. 2E). This data showed that Retro-2-dependent STxB–ss–saporin trafficking through the retrograde transport route was conserved in THP-1 cells.

STxB–ss–saporin translocates from an endosomal compartment to the cytosol

To gain further insight into the intracellular pathways by which STxB reaches the cytosol, we compared the intoxication capacity of the STx-1 holotoxin to that of the covalent reducible STxB–ss–saporin conjugate in control cells and under conditions of inhibition of retrograde transport by Retro-2. As described previously (Stechmann et al., 2010), we found that Retro-2 protected HeLa cells when these were incubated with increasing doses of STx-1 (Fig. 3A). EC$_{50}$ values were obtained from dose–response intoxication curves, and the ratio between EC$_{50}$ values obtained in control and Retro-2-treated conditions was expressed as a protection factor. We thus found that upon Retro-2 treatment, STx-1 toxicity was reduced by 24.84±2.85-fold (mean±s.e.m., n=4, two independent experiments) after a 4-h toxin challenge on HeLa cells (Fig. 2E). Hence, these results indicate that retrograde transport inhibition is translated into reduced toxin arrival at its cytosolic target (a shift in EC$_{50}$, i.e. high protection factor).

Intoxication analysis demonstrated that Retro-2 was likewise able to protect THP-1 cells against intoxication with STx-1 (Fig. 3B). STx-1 toxicity on Retro-2-treated cells was reduced by 14.16±2.02 -fold (mean±s.e.m., n=6, three independent experiments) after a 4-h toxin challenge (Fig. 3E). These protective factor results again show that retrograde transport to the dislocation-competent ER compartment was efficiently blocked in both HeLa and THP-1 cells.

In contrast to STx-1 holotoxin, treatment with 25 µM Retro-2 did not significantly protect HeLa or THP-1 cells against STxB–ss–saporin (Fig. 3C,D). After a 4-h STxB–ss–saporin incubation, a negligible protection factor of 1.27-fold±0.78 (mean±s.e.m., n=4, two independent experiments) was observed on HeLa cells upon retrograde transport inhibition, and of 0.51-fold±0.09 (mean±s.e.m., n=4, two independent experiments) on THP-1 cells (Fig. 3E). During the course of our study, structure–activity relationship (SAR) studies focusing on Retro-2 optimization lead to cyclic analogues with an ~100-fold improvement in the EC$_{50}$ against Shiga toxin (Noel et al., 2013). We therefore also investigated whether inhibition of retrograde transport through an improved (i.e. more bioactive) Retro-2 molecule (denoted Retro-2 cycl) could inhibit STxB–ss–saporin cytosolic translocation. Calculation of the

fold change in the EC$_{50}$ (protection factor) demonstrated that upon Retro-2 cycl treatment and a 4-h toxin challenge, STx-1 toxicity was reduced by 54.58±25.23-fold (mean±s.e.m., n=4, two independent experiments) on Hela cells and 34.51±13.29-fold (mean±s.e.m., n=4, two independent experiments) on THP-1 cells (Fig. 3F). In contrast, treatment with Retro-2 cyl did not protect HeLa or THP-1 cells against STxB–ss–saporin, with negligible protection factors of 2.10±0.15 (mean±s.e.m., n=4, two independent experiments) and 1.30±0.20 (mean±s.e.m., n=4, two independent experiments), respectively (Fig. 3F).

Upon Retro-2 treatment, STxB has been shown to accumulate in an endosomal compartment labeled by the early endosomal marker EEA-1 (Stechmann et al., 2010). Our results showing that STxB–ss–saporin-mediated toxicity remained unaffected when retrograde transport was inhibited by Retro-2 or the more potent Retro-2 cycl, therefore, suggested that this covalent toxin version translocated from early endosomes to reach its cytosolic target and to mediate protein biosynthesis inhibition.

Brefeldin A (BFA) is known to disrupt Golgi morphology and to protect cells from cytotoxic effects exerted by STx-1 holotoxin (Donta et al., 1995). Intoxication assays on HeLa cells confirmed that treatment with 5 µg/ml BFA indeed protected HeLa cells against a 4-h STx-1 challenge (Fig. 3G). In contrast, BFA treatment did not affect STxB–ss–saporin-mediated protein biosynthesis inhibition (Fig. 3H), supporting the notion that cytosolic translocation of STxB–ss–saporin is independent of retrograde transport to the Golgi and must occur from an endosomal compartment.

Next, we compared the intoxication of human monocyte-derived macrophages (HMDMs) with STx-1 and STxB–ss–saporin. It has previously been reported that, in contrast to toxin-sensitive HeLa or THP-1 cells, STx-1 does not intoxicate HMDMs (Falguières and Johannes, 2006). Furthermore, we have also shown in biochemical and morphological assays that STxB cannot be detected along the retrograde route in these cells, demonstrating that targeting of STxB to the Golgi and ER did not measurably occur (Falguieres et al., 2001). Rather, STxB was transported to the late endosomal pathway, where the protein was degraded. Intoxication curves after 24 h confirmed that HMDMs were indeed insensitive to STx-1, as no decrease in protein biosynthesis was observed (Fig. 4A). In contrast, STxB–ss–saporin intoxicated HMDMs, as shown by the clear dose-dependent curve with an EC$_{50}$ value of 0.22 ng/ml that was obtained after a 24-h STxB–ss–saporin challenge (Fig. 4B). STxB–ss–saporin thus intoxicated cells in which STxB is not detectably targeted to the retrograde route.

Cross-presentation of CD8+ epitopes derived from CMV

To test the role of retrograde transport in STxB-mediated antigen cross-presentation, we generated a conjugate between STxB and the human Cytomegalovirus (CMV) human leukocyte antigen (HLA)-A2-restricted CMV$_{495–503}$ peptide. CD8$^+$ T cells against CMV$_{495–503}$ were induced in humans, as previously described (Godard et al., 2004). THP-1 cells were pre-incubated with Retro-2 (black bars; Fig. 4C,D) or DMSO (gray bars), and then pulsed with 2 µg/ml or 20 µg/ml of STxB–CMV$_{495–503}$ conjugate. After 2 h, 50,000 (Fig. 4C) or 25,000 (Fig. 4D) anti-CMV CD8$^+$ T cells were added and co-cultured with THP-1 cells for an additional 20 h. After washing, the production of interferon γ (IFNγ), a marker of the activation of anti-CMV CD8$^+$T cells after HLA-A2–CMV$_{495–503}$ complex recognition, was monitored by the IFNγ Elispot technique. As negative controls, we used wells without cells, or wells with cells that had not been pulsed with antigen. As a positive control, we
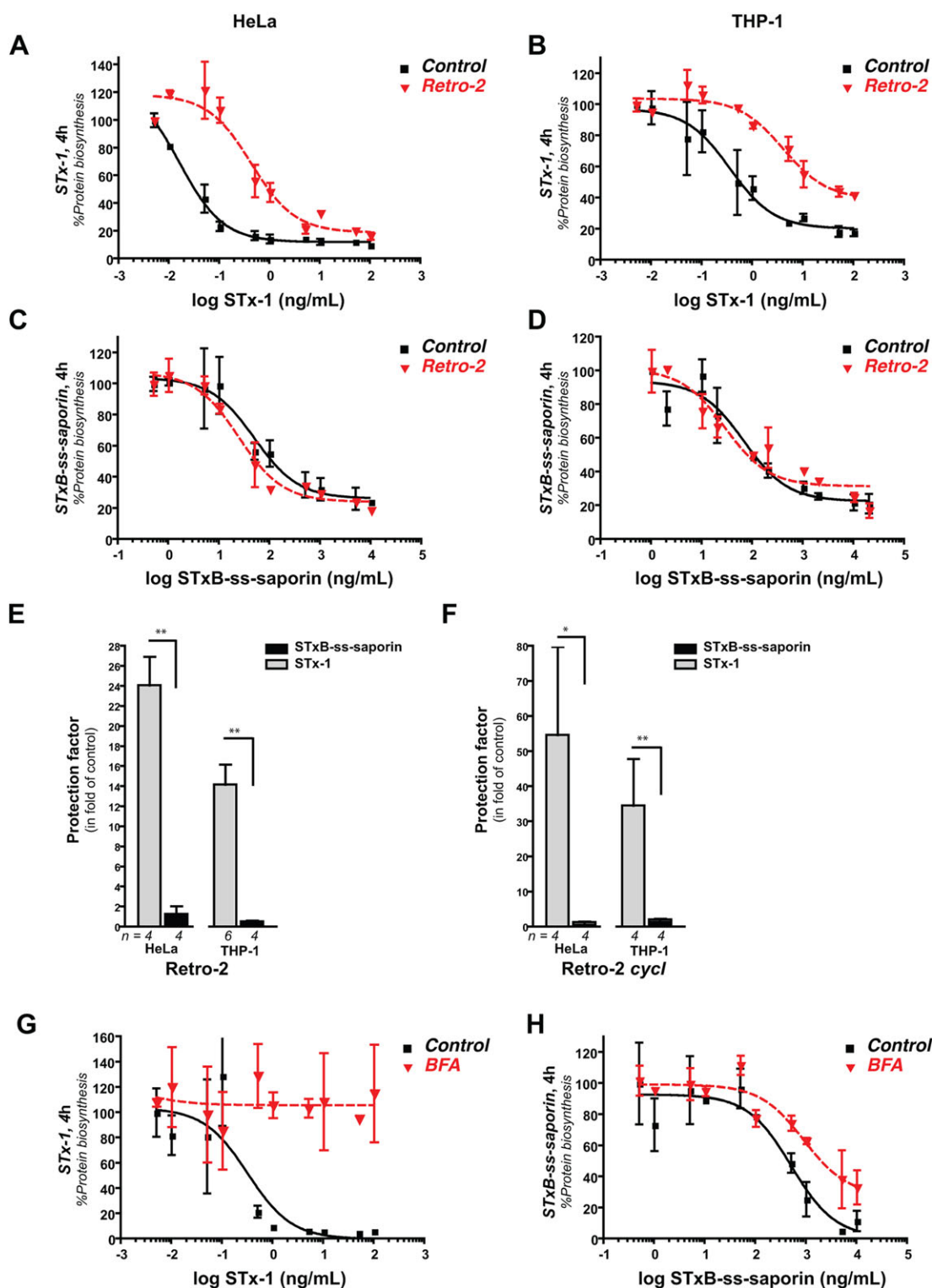
Fig. 3. Retro-2 does not prevent STxB–ss–saporin-mediated toxicity. (A–F) Retro-2 effect of cell intoxication. HeLa or THP-1 cells were pre-treated with 0.05% DMSO (black curves) or 25 µM Retro-2 (red curves) for 30 min prior to a 4-h exposure to STx-1 (A,B) or STxB–ss–saporin (C,D). Results for A–D are mean±s.e.m. from a representative experiment in duplicate. Protection factors for experiments with Retro-2 (E) and Retro-2 cyl (F) were determined for the indicated number of replicates from two or three independent experiments. Data are means±s.e.m. *P<0.05, **P<0.01, unpaired one-tailed Student's t-test. (G,H) BFA effect of cell intoxication. HeLa cells were pre-treated or not with 5 µg/ml BFA for 30 min prior to a 4-h incubation with increasing doses of (G) STx-1 or (H) STxB–ss–saporin. Note that BFA protected cells efficiently against STx-1, but not against STxB–ss–saporin. Results are mean±s.e.m. from a representative out of two independent experiments in duplicate.

pulsed THP-1 cells with free CMV$_{495\text{-}503}$ peptide. As shown in Fig. 4C,D, in none of the experimental conditions did Retro-2 affect the HLA-class I-restricted presentation of the CMV peptide.

We, therefore, conclude that STxB–CMV$_{495\text{-}503}$ is also translocated in a Retro-2-insensitive manner to the cytosol, most likely from endosomes.
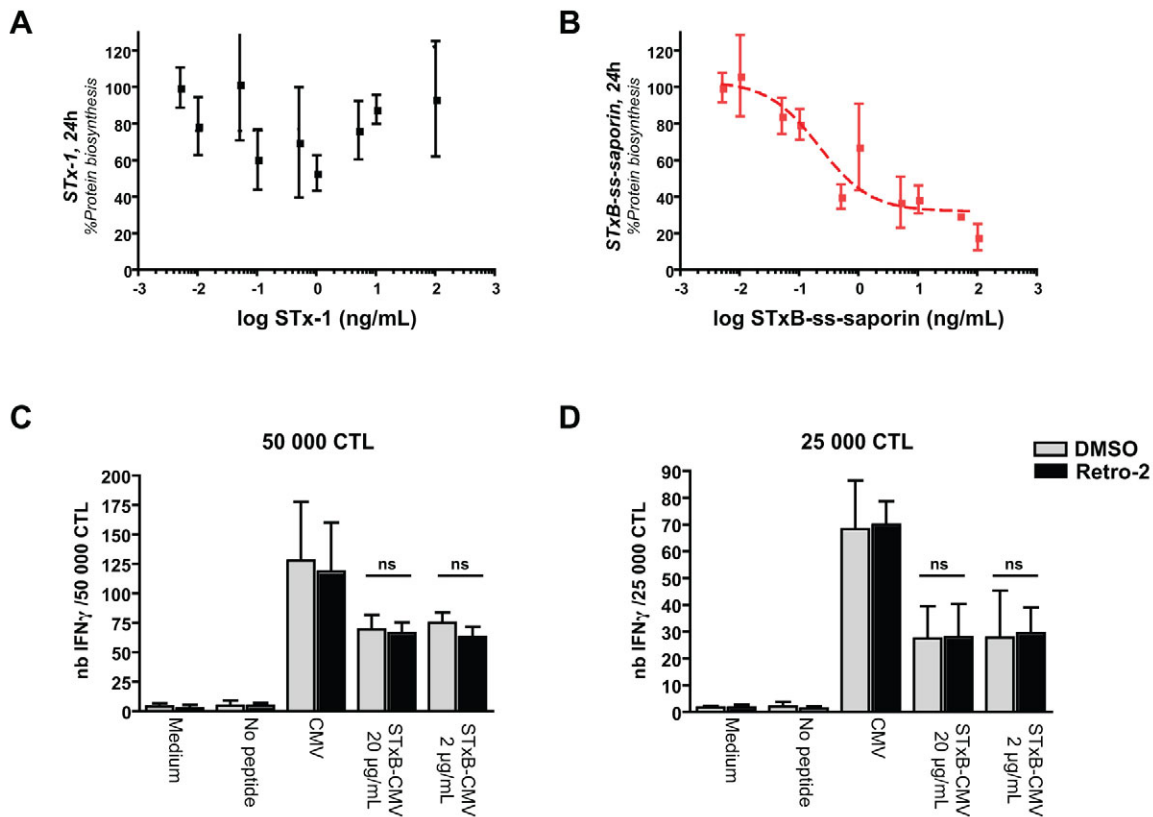
Fig. 4. Retro-2 does not affect cross-presentation. (A,B) Intoxication assays on HMDM after a 24-h challenge with (A) STx-1 or (B) STxB–ss–saporin. Results are mean±s.e.m. from a representative out of two independent experiments in duplicate. (C,D) Cross-presentation assay. In an IFNγ Elispot plate, THP-1 cells were pre-incubated for 30 min with 0.05% DMSO (gray bars) or 25 μM Retro-2 (black bars) and pulsed for 2 h with STxB–CMV$_{495–503}$ (2 μg/ml or 20 μg/ml), or free CMV$_{495–503}$ peptide. Anti-CMV$_{495–503}$ HLA-A2-restricted CTL were added [50,000 (C), or 25,000 (D)] and co-cultured with THP-1 cells for 20 h. IFNγ-spot-forming cells were detected as per the manufacturer's instruction. Results correspond to mean±s.e.m. for four replicates of two independent experiments. ns, not significant (two-tailed Mann–Whitney U-test).

Functional dissection of endosomal escape

Targeting of STxB through the retrograde transport to the ER has previously been shown to operate in association with detergent-resistant membranes (DRMs), and cholesterol extraction inhibited STxB transport at the early-endosome–TGN interface (Falguieres et al., 2001). To study the effect of cholesterol on STxB–ss–saporin trafficking, HeLa cells were treated with 5 mM methyl-β-cyclodextrin (MβCD) for 30 min prior to the addition of STxB or STxB–ss–saporin for 45 min at 37°C. In mock-treated cells, colocalization of STxB (red; Fig. 5A, left column) or STxB–ss–saporin (red; Fig. 5C, left column) with giantin (green) was indicative of STxB trafficking to the Golgi. In contrast, when cells were pre-treated with MβCD, the overlap between STxB (Fig. 5A, right column) or STxB–ss–saporin (Fig. 5C, right column) and giantin was strongly reduced, confirming that STxB transport was inhibited. The colocalization between STxB and giantin was quantified in all cases, as indicated (Fig. 5B,D).

To assess the effect of cholesterol depletion on cytosolic translocation, intoxication analysis was performed on HeLa cells that were pretreated or not with 5 mM MβCD before a 4-h incubation with STx-1 or STxB–ss–saporin. In line with our immunofluorescence experiments, analysis of EC$_{50}$ values from dose–response intoxication curves after a STx-1 challenge (Fig. 5E) revealed a protection factor of 5.49±1.16-fold in MβCD-treated cells (mean±s.e.m., n=5, three independent experiments) (Fig. 5G). Strikingly, we found that cholesterol extraction did not inhibit, but

rather strongly sensitized cells to STxB–ss–saporin (Fig. 5F), with a protection factor of 0.21±0.38-fold (mean±s.e.m., n=7, four independent experiments, Fig. 5H; note that a protection factor <1 indicates sensitization), reflective of a significant increase in cellular toxicity. Qualitatively similar results were obtained when zaragozic acid was used to inhibit sterol synthesis (Fig. 5G,H). These findings point to a previously unrecognized link between cellular cholesterol levels and endosomal escape to the cytosol, support our data on retrograde transport inhibition with Retro-2 or brefeldin-A and establish that arrival to an endosomal compartment is indeed sufficient for the cytosolic translocation of STxB–ss–saporin.

We also used a well-characterized temperature block to examine STxB–ss–saporin translocation to the cytosol. In a previous study, we have shown that STxB transport to the Golgi is blocked at 19.5°C, and that STxB accumulates in early endosomes in these conditions (Mallard et al., 1998). Intoxication assays after a 4-h exposure to STx-1 holotoxin demonstrated that at 19.5°C, the sensitivity of HeLa cells to STx-1-induced protein biosynthesis was indeed reduced, with a protection factor of 7.63±0.73 (mean±s.e.m., n=4, two independent experiments) (Fig. 5G; supplementary material Fig. S3A, left panel). The effect was even stronger for STxB–ss–saporin for which the curves did not converge and the EC$_{50}$ value could not be determined (Fig. 5H; supplementary material Fig. S3A, right panel). Hence, the 19.5°C temperature block not only impacted trafficking along the retrograde route, but had an even stronger effect on STxB–ss–saporin translocation across endosomal membranes.
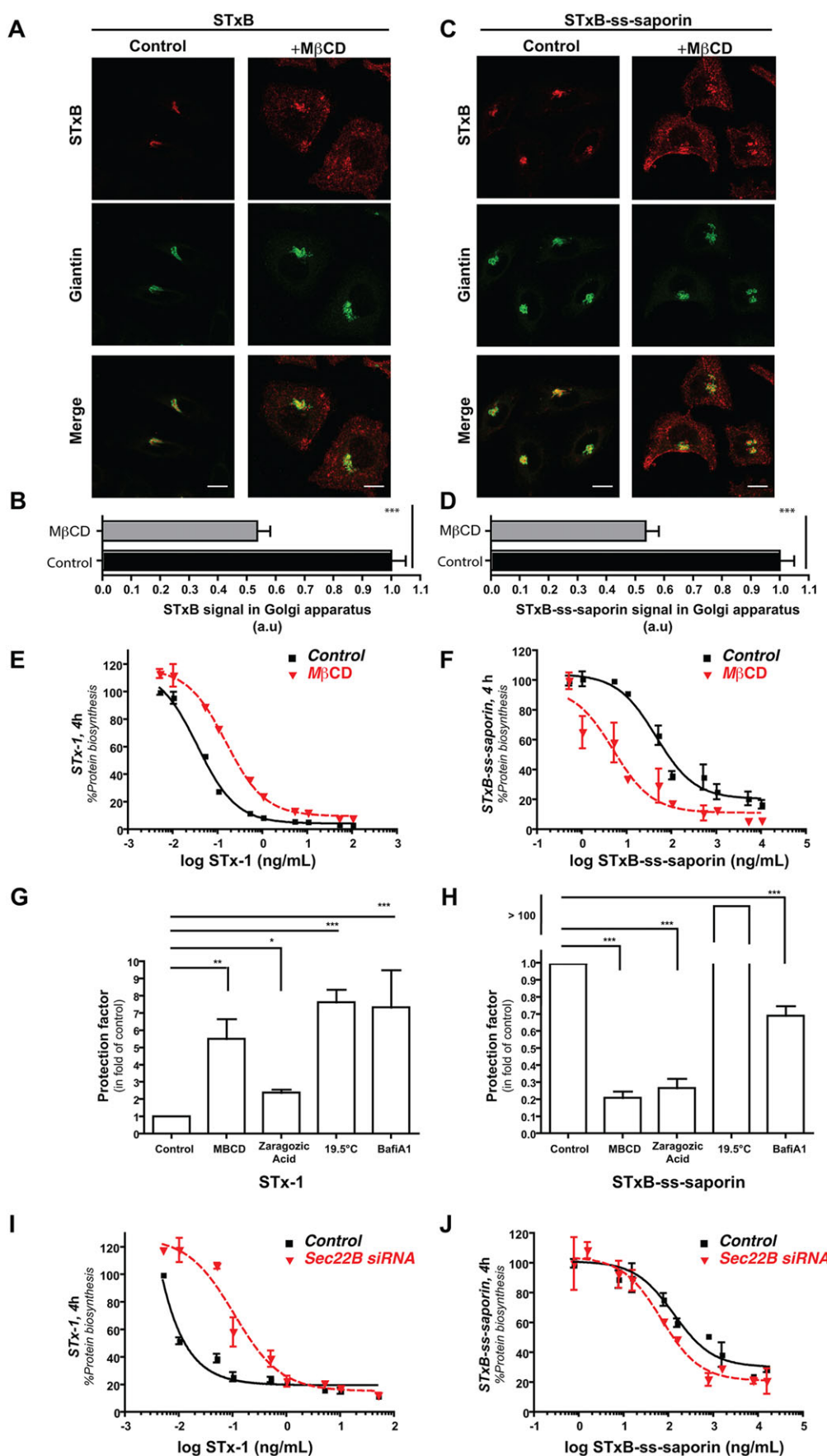
Fig. 5. See next page for legend.

Fig. 5. Cholesterol effect on STxB–ss–saporin-mediated protein biosynthesis inhibition. (A–D) Retrograde transport in MβCD-treated cells. (A) STxB or (C) STxB–ss–saporin were bound on ice to control or cholesterol-depleted (+MβCD) HeLa cells, which were then incubated for 45 min at 37°C, fixed and imaged by confocal microscopy after labeling for STxB (red) and giantin (green). In both cases, STxB signal in the Golgi area was quantified. For STxB (B), 1 arbitrary unit (a.u.) corresponds to 59.22±2.25% of STxB in Golgi area. Control n=56 cells, MβCD n=45 cells. For STxB–ss–saporin (D), 1 a.u. corresponds to 29.14±1.45% of STxB in Golgi area. Control n=46 cells, MβCD n=50 cells. Results are means±s.e.m. from two independent experiments. ***P<0.001 (unpaired Student's t-test). Scale bars: 10 µm. (E,F) Representative intoxication experiment after a 4-h exposure to (E) STx-1 or (F) STxB–ss–saporin in control cells (black curves), or after cholesterol extraction (red curves). (G,H) Protection factors after a 4-h STx-1 (G) or STxB–ss–saporin (H) challenge. For each toxin, four to eight replicates were analyzed per condition, from two to four independent experiments. Data are means±s.e.m. *P<0.05, **P<0.01, ***P<0.001 (ANOVA with Bonferroni's multiple comparison test). (I,J) Intoxication assays on Sec22B-depleted HeLa cells are shown after a 4-h (I) STx-1 or (J) STxB–ss–saporin challenge. Results are mean±s.e.m. and are representative of two independent experiments.

These findings utilizing cholesterol depletion and temperature block support our initial conclusions on two different membrane translocation mechanisms that discriminate the non-covalent (STx-1 holotoxin) and covalent (STxB–ss–saporin) toxin versions, and provide further evidence that STxB–ss–saporin translocated from endosomes to the cytosol.

Several groups have reported that limiting endo-phagosomal acidification enhances antigen cross-presentation (Jancic et al., 2007; Savina et al., 2006, 2009). We therefore examined whether the efficacy of cytosolic translocation of STxB–ss–saporin was altered in an alkaline endosomal environment. Bafilomycin A1, an inhibitor of endosomal acidification, is known to slow early-endosome-to-TGN transport, and to protect cells against STx (Dyve Lingelem et al., 2012). In our hands, bafilomycin A1 treatment of HeLa cells also led to a 7.34±2.14-fold protection (mean±s.e.m., n=6, three independent experiments) against STx-1 holotoxin (Fig. 5G; supplementary material Fig. S3B, left panel). In contrast, the protection factor value was 0.69±0.06 (mean±s.e.m., n=8, four independent experiments) in bafilomycin-A1-treated Hela cells that were exposed to increasing concentrations of STxB–ss–saporin (Fig. 5H; supplementary material Fig. S3B, right panel), reflective of a significant increase in toxicity, or, in other words, an increase in STxB–ss–saporin arrival to the cytosol, implying that endosomal pH is indeed a crucial factor in this process.

In the ER–phagosome fusion antigen cross-presentation model, one of the specific features of the cross-presenting compartment is the recruitment of ER-resident proteins, involving the ER SNARE protein Sec22B (Cebrian et al., 2011). Sec22B was depleted using small interfering RNAs (siRNAs) to examine its possible role in the translocation of STxB–ss–saporin to the cytosol. Such Sec22B-depleted cells (supplementary material Fig. S4A) were strongly protected against STx-1 holotoxin (Fig. 5I), likely because of an inhibitory effect in retrograde transport at the Golgi–ER interface (Lewis et al., 1997). However, the protein biosynthesis inhibition by STxB–ss–saporin was not affected in Sec22B-depleted cells (Fig. 5J). These results, hence, suggest that Sec22B function is not a prerequisite for the translocation of STxB–ss–saporin to the cytosol.

Rab proteins belonging to the Ras superfamily of small GTPases play a crucial role in regulating membrane trafficking. Therefore, we decided to further investigate this protein family to gain insight as to the nature of the translocation-competent compartment. Previous studies have shown that the Golgi-associated GTPase Rab6a, and more specifically the Rab6a′

isoform, regulates early-endosome-to-TGN transport (Del Nery et al., 2006; Mallard et al., 2002). HeLa cells were treated with control siRNAs or siRNAs targeting Rab6a′, Rab6a, or both isoforms, as described previously (Del Nery et al., 2006). Efficient silencing of both Rab6 isoforms was confirmed at the level of protein expression by western blot analysis using a pan-specific antibody (supplementary material Fig. S4B). Only cells depleted for Rab6a′ were significantly protected against intoxication by STx-1 holotoxin (Fig. 6A), with a measured protection factor of 13.57±3.40-fold (mean±s.e.m., n=4; two independent experiments) (Fig. 6G). In contrast, STxB–ss–saporin-mediated toxicity remained unaffected by inhibition of retrograde transport achieved by depletion of Rab6a′ (Fig. 6B,G), confirming that retrograde transport and Rab6a′ activity are not required for the cytosolic translocation of STxB–ss–saporin.

Rab5 has been consistently ascribed a multitude of functions in endocytosis (Semerdjieva et al., 2008) and at the early endosome (reviewed in Mohrmann and van der Sluijs, 1999). We therefore also examined whether Rab5 could play a role in the cytosolic translocation of STxB. We used siRNAs to efficiently deplete Rab5 from HeLa cells (supplementary material Fig. S4C). After a 4-h STx-1 challenge on HeLa cells, an EC_{50} could not be measured as cytotoxicity curves did not converge (Fig. 6C,G), demonstrating that Rab5-depleted cells were strongly protected against the holotoxin. By contrast, however, these cells were not protected against the STxB–ss–saporin conjugate (Fig. 6D,G).

The transition from early to late endosomes has been described as a loss of Rab5 and its effector EEA1 from endosomal carrier vesicles, with the simultaneous recruitment of Rab7. As Rab7 has been implicated in the regulation of transport along the endo-lysosomal pathway (Ceresa and Bahr, 2006; Vanlandingham and Ceresa, 2009), we examined whether Rab7 could play a role in STxB–ss–saporin translocation. We used siRNAs to deplete Rab7 from HeLa cells for 72 h, as previously described (Girard et al., 2014) (supplementary material Fig. S4D). After a 4-h challenge with STx-1 holotoxin (Fig. 6E), a slight protection factor of 1.76±0.04 (mean±s.e.m., n=4, two independent experiments) was measured (Fig. 6G). In contrast, protection against intoxication with STxB–ss–saporin conjugate was increased by 10.31±2.9-fold 8 (mean±s.e.m., n=4, two independent experiments) after Rab7 depletion (Fig. 6F,G), strongly suggesting that in the absence of Rab7, the translocation of STxB–ss–saporin to the cytosol is inhibited.

Reducible versus non-reducible linker arms
The STxB–ss–saporin conjugate that was used up to this point contained a cleavable disulfide linker arm. Surprisingly, incubation of HeLa or THP-1 cells with a covalent conjugate that did not contain the reducible linker arm (termed STxB–saporin) did not lead to inhibition of protein biosynthesis (Fig. 7A). Given that this conjugate is catalytically active (see supplementary material Fig. S1C), it can be concluded that saporin did not reach ribosomes in the non-cleavable configuration.

To analyze whether this was due to a lack of membrane translocation to the cytosol or due to a deficiency to shuttle from the site of membrane translocation across the cytosol to ribosomes, we replaced saporin by another enzyme, β-lactamase, yielding STxB–ss–β-lactamase and STxB–β-lactamase. β-lactamase catalyzes the cleavage of a cephalosporin-derived CCF4-based fluorescence resonance energy transfer (FRET) reporter, leading to a loss of FRET signal that can be quantified (Keller et al., 2013; Ray et al., 2010; Simeone et al., 2012). CCF4-AM is an esterified, membrane permeable form of the CCF4 substrate which specifically
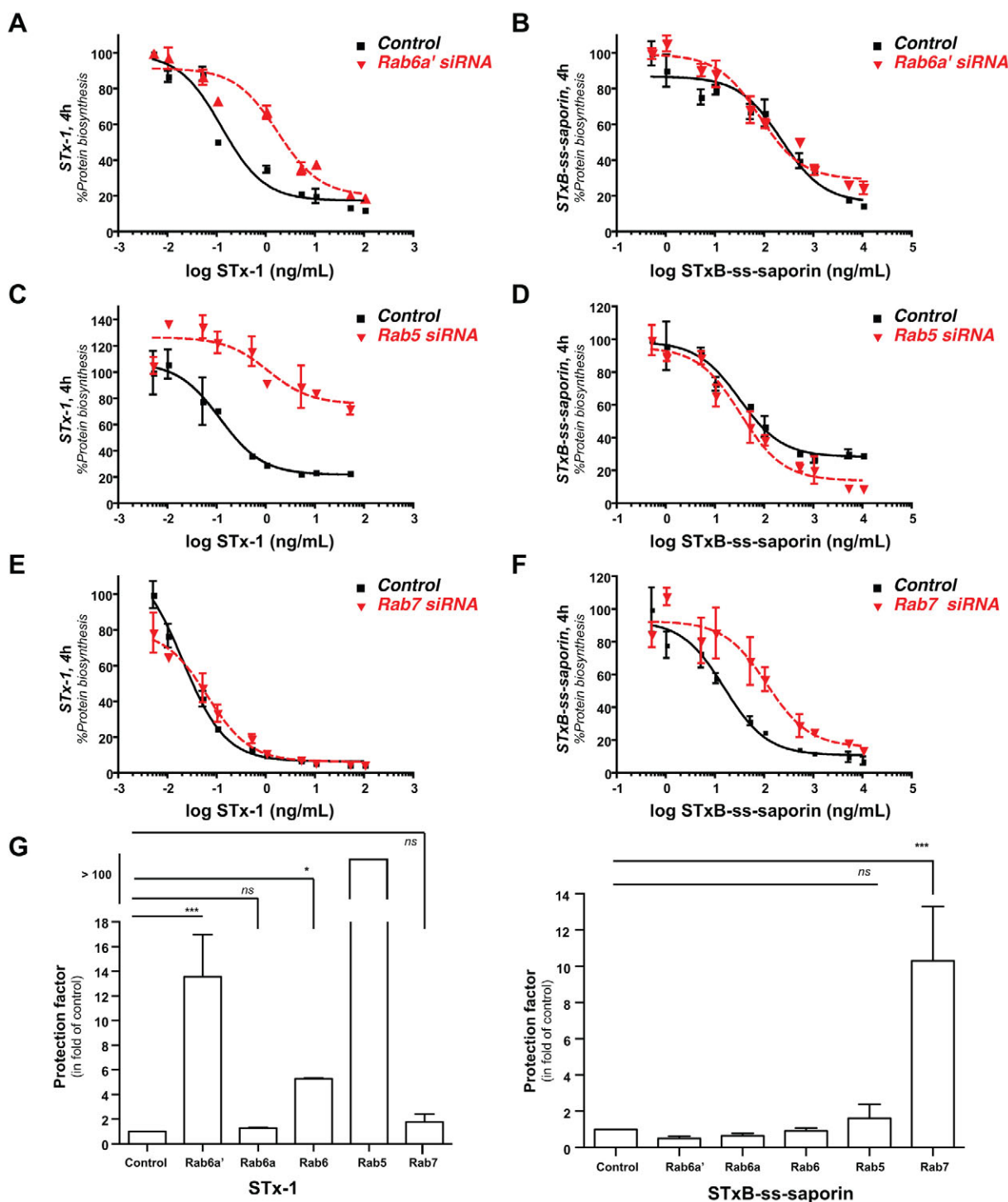
Fig. 6. STxB-ss-saporin-mediated protein biosynthesis inhibition is Rab7-dependent. HeLa cells were challenged for 4 h with STx-1 (A,C,E) or STxB–ss–saporin (B,D,F) in control conditions (black curves), or after (A,B) Rab6a′, (C,D) Rab5 or (E,F) Rab7 depletion (red curves). Results are mean±s.e.m. from a representative experiment in duplicate. (G) Protection factors (means±s.e.m.) are shown for four replicates from two independent experiments. *P<0.05; ***P<0.001; ns, not significant (ANOVA with Bonferroni's multiple comparison test).

equilibrates in the cytosol of host cells after cytoplasmic esterase cleavage. The advantage of this configuration is that, in comparison to the saporin reporter, β-lactamase does not need to diffuse across the cytosol to meet its substrate.

THP-1 cells were loaded with CCF4-AM, and then incubated for 3 h with unconjugated β-lactamase, with disulfide cleavable STxB–ss–β-lactamase, or with non-cleavable STxB–β-lactamase.

A loss of FRET leading to an increased emission at 450 nm was observed with both conjugates used at 30 μg/ml, and to a much lesser extent with 30 μg/ml unconjugated β-lactamase (Fig. 7B). This data was quantified by calculating the fluorescence intensity ratiometric values for 450 nm to 535 nm in all conditions (Fig. 7C). It was thereby confirmed that disulfide-cleavable STxB–ss–β-lactamase and non-cleavable STxB–β-lactamase were
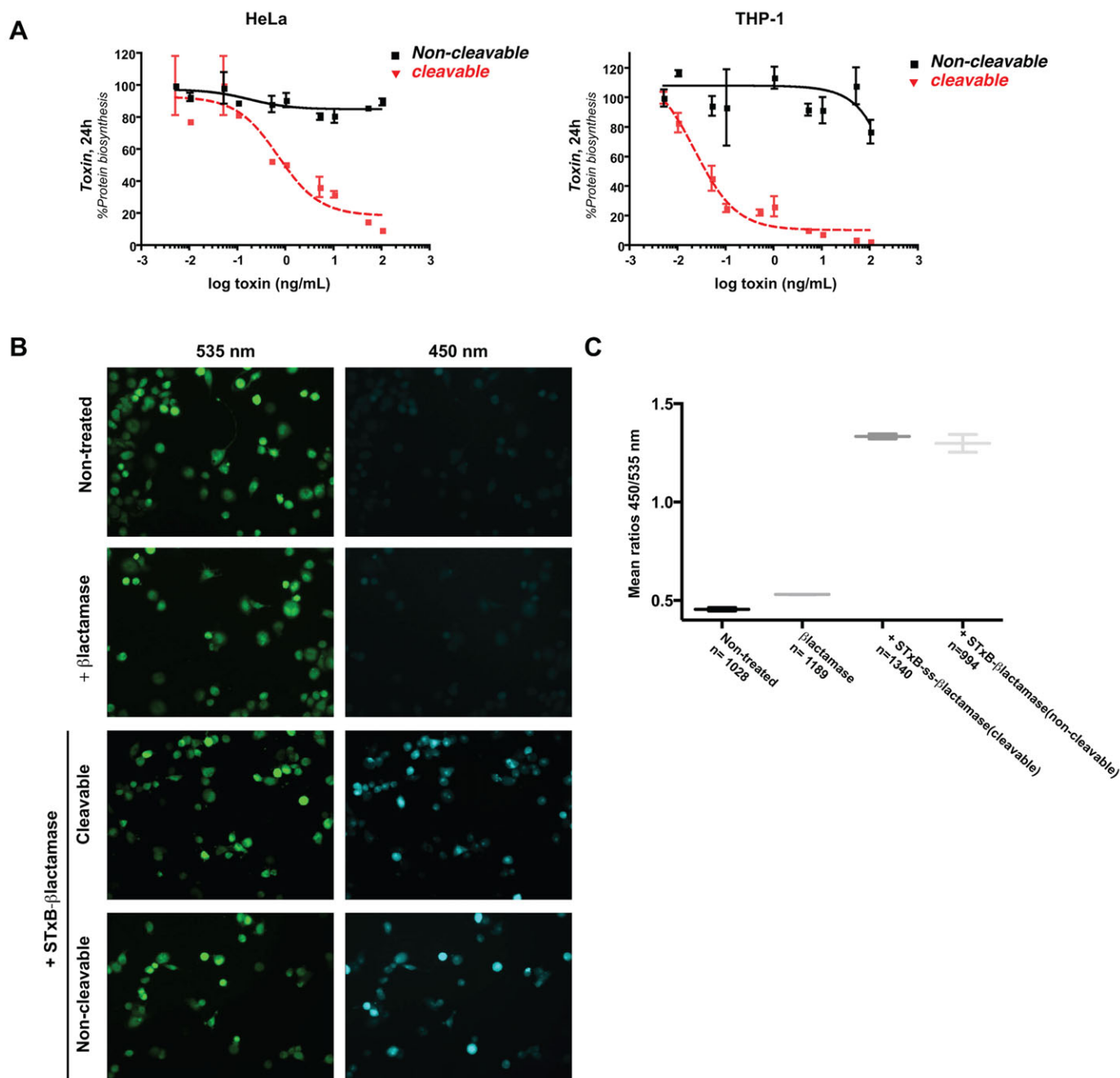
Fig. 7. FRET-based export assay to the cytosol. (A) Intoxication curves after a 24 h incubation of disulfide-cleavable STxB–ss–saporin (red curves) or non-cleavable STxB–saporin (black curves) with HeLa (left panel) or THP-1 (right panel) cells. Results are mean±s.e.m. from one representative out of three independent experiments in duplicate. (B,C) β-lactamase assay. CCF4-AM-loaded THP-1 cells were incubated for 3 h with 30 µg/ml of unconjugated β-lactamase, or 30 µg/ml STxB coupled to β-lactamase through cleavable (STxB–ss–β-lactamase) or non-cleavable (STxB–β-lactamase) linker arms, and analyzed by confocal microscopy. (B) Representative images were chosen for the following channels: the intact CCF4 probe at 535 nm (green) and the cleaved CCF4 probe at 450 nm (blue). (C) Histogram shows the outcome of post-acquisition analysis. The ratio of the 450 nm to 535 nm mean fluorescence intensity was quantified over the indicated number of cells. Means±s.e.m. of two independent experiments.

both equally efficient at increasing the 450 nm to 535 nm ratio. These data, hence, suggest that the difference that was observed in the protein biosynthesis inhibition experiments with disulfide cleavable STxB–ss–saporin and non-cleavable STxB–saporin was not due to a deficiency in cytosolic export, but rather due to differences in their ability to reach their ribosomal target once they were localized on the cytosolic side of endosomal membranes.

DISCUSSION

The mechanisms by which antigens are transferred to the cytosol for cross-presentation are amongst the least well understood in cell biology. Using the STxB-driven cross-presentation model, we demonstrate that retrograde transport is not required for cytosolic escape, and that Rab7 and cholesterol are involved. We also report evidence for the association of STxB with the cytoplasmic leaflet after membrane translocation.

One outstanding issue regarding STxB-mediated antigen cross-presentation was the question of whether retrograde transport was required. Addressing this aspect has become possible because of the availability of the highly specific Retro-2 compound that inhibits retrograde STxB trafficking at the early-endosome–TGN interface, but leaves other intracellular transport events unaffected, including the biosynthetic and secretory pathway (Stechmann et al., 2010). The selective effect of Retro-2 on STx-1 holotoxin, but not the STxB–ss–saporin or STxB–CMV$_{495-503}$ conjugates, strongly suggests that translocation to the cytosol of the covalent version of the toxin occurs from an endosomal compartment. The finding that BFA also did not affect cell intoxication by STxB–ss–saporin further reinforces this conclusion. This situation is similar to the one described for other cross-presentation modalities where it was equally suggested that specifically the early endocytic pathway was of importance (Belizaire and Unanue, 2009; Burgdorf et al., 2007, 2008), which is exclusively targeted by STxB (Mallard et al., 1998).

The finding that depletion of Rab5 did not affect cell intoxication by STxB–ss–saporin was surprising, when considering the central function of this GTPase on early endosomes (see Shin et al., 2005 and references therein). In contrast, Rab7 depletion clearly decreased STxB–ss–saporin-driven protein biosynthesis inhibition. Rab7 has lately been shown to have a number of functions in addition to regulating trafficking in the late endocytic pathway (Bucci et al., 2000), such as retrograde sorting (Rojas et al., 2008), endosome–phagosome fusion (Becken et al., 2010) and cholesterol trafficking (Girard et al., 2014). Whether the effect of Rab7 on endosomal escape of STxB is direct, or is indirect and modulated by a general membrane parameter such as cholesterol homeostasis, remains to be analyzed.

The stimulatory effect on endosomal escape of STxB upon interference of cholesterol homeostasis is another striking finding of this study. Although it cannot be mechanistically interpreted at this stage, it is of interest to note that lipid domains have been linked to the process of membrane permeability. First, it has been well established for many years that the ion permeability of membranes dramatically increases at domain boundaries owing to structural defects and mismatches in the molecular packing (see Cruzeiro-Hansson and Mouritsen, 1988 and references therein). Second, more recent work has described a defect in cross-presentation of phagocytosed antigens in cells in which lipid droplet biogenesis was impaired (Bougnères et al., 2009). Lipid pores are associated with droplet biogenesis, and it has been suggested that pore formation would be favored by lipids with a bulky head groups (Ploegh, 2007) and STxB precisely binds to such bulky head group lipids (i.e. the glycosphingolipid Gb3). Our study thereby points to a possible link between membrane cholesterol levels, glycolipid domain formation and membrane translocation. The exquisite sensitivity of cell intoxication by STxB–ss–saporin to incubation at 19.5°C is also an indirect indicator that lipid domain formation has a role in endosomal membrane translocation.

The differential sensitivity of STxB conjugates with saporin or β-lactamase with respect to the nature of the linker arm was surprising. Although β-lactamase was equally efficient at transforming its cytosolic substrate (i.e. a CCF4-based FRET reporter) when linked to STxB by a disulfide-cleavable or non-cleavable linker arms, saporin was able to intoxicate cells only when linked to STxB by the disulfide-cleavable linker arm. The most likely interpretation of this finding is that STxB remains associated with the cytosolic leaflet after its translocation across the endosomal membrane. In such a configuration, ribosomes on the ER could only be reached if saporin was dissociated from STxB. In contrast,

β-lactamase would be reached by its freely diffusible FRET reporter substrate even if it was permanently associated with STxB on the cytosolic endosome membrane leaflet. These findings are more readily explained by the lipid pore hypothesis in which STxB remains associated with its glycosphingolipid receptor while flipping across the membrane. In contrast, a protein pore would necessarily require a dissociation between the Gb3 receptor and STxB, leaving unexplained a subsequent re-association with the membrane once the cytosol is reached.

In conclusion, our current findings provide a fresh perspective on the endosomal escape question, and are expected to provide new directions for membrane biology research in the field of antigen cross-presentation.

MATERIALS AND METHODS
Cell lines
The human monocytic THP-1 cell line was cultured at 37°C under 5% CO_2 in RPMI medium (Invitrogen), supplemented with 10% heat-inactivated fetal bovine serum (Pan Biotech), 0.01% penicillin-streptomycin (Invitrogen), 4 mM L-glutamine and 5 mM sodium pyruvate. THP-1 differentiation and adherence was induced by overnight treatment with 160 nM 12-O-tetradecanoylphorbol-13-acetate (TPA) (Cell Signaling) as described previously (Uchide and Toyoda, 2007).

HeLa cells were maintained at 37°C under 5% CO_2 in Dulbecco's modified Eagle's medium (DMEM, Invitrogen), supplemented with 10% heat-inactivated fetal bovine serum, 0.01% penicillin-streptomycin, 4 mM glutamine and 5 mM pyruvate. In addition, the medium was supplemented with 0.5 mg/ml G418 for HeLa cells stably expressing endoA2–GFP.

Human monocytes were isolated from human blood of healthy donors on ficoll density gradients (Eurobio, les Ulis, France), and subsequently differentiated into macrophages (HMDM) for 7 days in RPMI medium, supplemented with 10% heat-inactived fetal bovine serum, 2 mM glutamine, 100 UI/ml penicillin, 100 µg/ml streptomycin, and 20 ng/ml human macrophage colony-stimulating factor (hM-CSF; AbCys, Paris, France).

Drug treatments
For treatment with Retro-2 or Retro-2 cycl, HeLa or THP-1 cells were pre-treated for 30 min at 37°C with 25 µM Retro-2 or Retro-2 cycl, which was diluted in the corresponding growth medium. Retro-2 {2-([(5-methyl-2-thienyl)methylene]amino)-N-phenylbenzamide} was purchased from Chembridge (San Diego, CA) and was also synthesized in-house. Similarly, HeLa cells were pre-treated for 15 min with 5 µg/ml BFA, 30 min with 500 nM bafilomycin A1 or 30 min with 5 mM MβCD (all purchased from Sigma) prior to the addition of STx-1 or STxB–ss–saporin for 4 h. Cells for zaragozic acid experiments were cultured for 24 h in DMEM supplemented with 10% lipid-deficient serum and with 50 µM zaragozic acid (Tebu-Bio SA, Le Perray-en-Yvelines, France) prior to toxin addition.

Immunofluorescence, confocal and TIRF imaging
Control or Retro-2-treated cells were incubated with 0.5 µg/ml STxB or STxB–ss–saporin on ice for 30 min, followed by 45 min at 37°C in the continued presence of vehicle or compound. Cells were fixed and immunolabeled with the indicated antibodies. Samples were imaged on a Ti inverted Nikon microscope fitted with a confocal A1R system, using a 60× oil immersion objective, NA 1.4. NIS Elements, MetaMorph (Molecular Devices) and ImageJ software (National Institutes of Health, Bethesda, MD) were used for image processing. Maximum projections of six to eight optical z-slices (250 nm z-separation) are shown.

STxB and STxB–ss–saporin were subjected to coupling with N-hydroxysuccinimide (NHS)-activated Cy3 as per the manufacturer's instructions (GE Healthcare). Plasma membrane images on living cells were then acquired on a total internal reflection fluorescence (TIRF) video microscope (Nikon) equipped with a CFI Apo TIRF 1003NA 1.49 oil objective and an EMCCD camera (PhotometricsHQ2).

Intoxication assay

Intoxication analysis of HeLa or TPA-treated THP-1 cells was performed as previously described (Stechmann et al., 2010). Briefly, 25,000 HeLa or 150,000 TPA-treated THP-1 cells per well were seeded into flat-bottomed 96-well optical plates (Nunc) and grown overnight at 37°C. Cells were incubated at 37°C for the indicated times with increasing doses of STx-1, STxB conjugates with saporin, or non-vectorized saporin. Then, cells were rinsed three times with PBS, and 1 μCi [^{35}S]-methionine (Perkin Elmer) was added for 60 min at 37°C to each well. Radiolabeled proteins were precipitated by washing cells three times with ice-cold 5% trichloroacetic acid and then three-times with PBS. Protein synthesis was quantified by liquid scintillation counting.

Results are expressed as percentages of incorporated radioactivity relative to the DMSO or scrambled siRNA control situations that were set to 100%. Protein biosynthesis levels as a function of toxin concentration was then fitted using GraphPad Prism software to obtain a non-linear dose–response curve from which EC_{50} values were obtained. To calculate protection factors, the EC_{50} values from n number of replicates were calculated, and the means were used to determine the ratio of the drug or siRNA EC50 to that of the control EC_{50}. For all representative intoxication curves that are shown, data are mean±s.e.m. from replicates of an independent experiment.

Sulfation assay

Sulfation analysis was performed on TPA-treated THP-1 cells as detailed previously (Amessou et al., 2006). 1 μM STxB-Sulf$_2$ was added to cells on ice for 30 min. Cells were washed with ice-cold PBS and incubated for 20 min at 37°C in DMEM supplemented with 480 μCi/ml [^{35}S]sulfate (Perkin Elmer). After cell lysis, STxB–Sulf$_2$ was immunoprecipitated using the monocolonal anti-STxB-13C4 antibody, separated on a Tris-Tricine gel, and quantified by autoradiography. To determine total sulfation counts, proteins were precipitated by adding 5% final concentration trichloroacetic acid. Precipitated proteins were then filtered on glass microfiber filters (Whatman), and filters counted using a Microbeta scintillation counter.

Immunofluorescence quantifications

Cy3-STxB fluorescence intensity was measured with ImageJ software (NIH) on z-projections, either from the entire cell, or from the Golgi region, as defined by giantin labeling. The ratio was then calculated as an index of Golgi localization.

N-glycosidase activity assay

20 μg of isolated yeast ribosomes (yeast strain ABYS1) were treated with increasing concentrations of unconjugated or STxB-coupled saporin for 1 h at 30°C in 1× Endo buffer (25 mM Tris-HCl pH 7.6, 25 mM KCl, 5 mM MgCl$_2$). The reaction was stopped, and rRNA was isolated by two phenol-chloroform extractions, and then precipitated. 4 μg of rRNA resuspended in water was treated for exactly 2 min at 60°C with acetic-aniline. rRNA was precipitated, resuspended in 60% de-ionized formamide with 0.1× TPE buffer, and separated on a denaturing formamide agarose gel. RNA fragments were quantified as described previously (Smith et al., 2003).

Antigen cross-presentation assay

Peripheral blood mononuclear cells (PBMCs) were extracted from peripheral blood of healthy HLA-A2 individuals by a standard ficoll density-gradient centrifugation. Informed consent was obtained from all of the participants. Total PMBCs were sensitized *in vitro* for 12 days by the addition of a specific CMV$_{495–503}$ peptide. IL-2 was added on days 3 and 7 (50 IU/ml, Chiron, Emeryville, CA). On day 12, THP-1 cells were pre-incubated with 25 μM Retro-2 (or 0.05% DMSO) for 30 min at 37°C, pulsed for 2 h with 20 μg/ml or 2 μg/ml STxB-CMV$_{495-503}$ or 10 μg/ml CMV$_{495–503}$, in the continued presence of 25 μM Retro-2 or 0.05% DMSO, and then co-cultured for 20 h with CMV-specific CD8+ CTL in a IFNγ coated Elispot plate (Diaclone), in the continued presence of 25 μM Retro-2 or 0.05% DMSO. IFNγ was detected as per the manufacturer's instructions. Elispot analysis was done with Immunospot Analyzer (Cellular Technology Limited).

β-lactamase assay

THP-1 cells were TPA-treated, and 150,000 cells per well seeded in 96-well plates 24 h prior to experiments. Adherent THP-1 cells were loaded with 1 mM of the CCF4-probe for 1 h. Then, cells were washed and incubated continuously for 3 h at 37°C with 30 μg/ml β-lactamase or 30 μg/ml STxB conjugates with β-lactamase prior to analysis by confocal microscopy. For details on acquisition and post-acquisition analysis, see the previous study by Keller et al. (Keller et al., 2013).

Quantification of colocalization with endoA2 using TIRF microscopy

To quantify the colocalization between two channels, an object-based method was used, as implemented in JACoP (Bolte and Cordelieres, 2006) based on the coincidence between two centroids with a 0.5-pixel tolerance (as described in Renard et al., 2015). This was achieved through an ImageJ macro by first segmenting the tagged proteins by spot detection in each channel, finding their position, and growing them by dilation to a 0.5-pixel radius. The spot detection consisted of finding maxima on the smoothed image (333 average filter) using the 'find maxima' plugin of ImageJ, whose noise tolerance parameter was set up visually independently for each channel. The results were expressed as the percentage of colocalized spots over the total number of spots in the red and the green channel, respectively.

Statistical testing

Statistical analysis was performed using Graph Pad Prism software. In the case of non-Gaussian distribution a two-tailed Mann–Whitney U-test was performed. The following parametric tests were used: one-tailed Student's t-test for the comparison of the means if there were only two conditions to compare or a parametric one-way ANOVA with a Bonferroni's multiple comparison test if there were more than two data groups to compare. Statistical significance is represented on the graphs by asterisks. All error bars denote s.e.m.

References

Ackerman, A. L., Kyritsis, C., Tampé, R. and Cresswell, P. (2005). Access of soluble antigens to the endoplasmic reticulum can explain cross-presentation by dendritic cells. *Nat. Immunol.* **6**, 107-113.

Ackerman, A. L., Giodini, A. and Cresswell, P. (2006). A role for the endoplasmic reticulum protein retrotranslocation machinery during crosspresentation by dendritic cells. *Immunity* **25**, 607-617.

Amessou, M., Popoff, V., Yelamos, B., Saint-Pol, A. and Johannes, L. (2006). Measuring retrograde transport to the trans-Golgi network. *Curr. Protoc. Cell Biol.* **32**, 15.10.1-15.10.21.

Badoual, C., Hans, S., Merillon, N., Van Ryswick, C., Ravel, P., Benhamouda, N., Levionnois, E., Nizard, M., Si-Mohamed, A., Besnier, N. et al. (2013). PD-1-expressing tumor-infiltrating T cells are a favorable prognostic biomarker in HPV-associated head and neck cancer. *Cancer Res.* **73**, 128-138.

Beaumelle, B., Alami, M. and Hopkins, C. R. (1993). ATP-dependent translocation of ricin across the membrane of purified endosomes. *J. Biol. Chem.* **268**, 23661-23669.

Becken, U., Jeschke, A., Veltman, K. and Haas, A. (2010). Cell-free fusion of bacteria-containing phagosomes with endocytic compartments. *Proc. Natl. Acad. Sci. USA* **107**, 20726-20731.

Belizaire, R. and Unanue, E. R. (2009). Targeting proteins to distinct subcellular compartments reveals unique requirements for MHC class I and II presentation. *Proc. Natl. Acad. Sci. USA* **106**, 17463-17468.

Bolte, S. and Cordelières, F. P. (2006). A guided tour into subcellular colocalization analysis in light microscopy. *J. Microsc.* **224**, 213-232.

Boucrot, E., Ferreira, A. P. A., Almeida-Souza, L., Debard, S., Vallis, Y., Howard, G., Bertot, L., Sauvonnet, N. and McMahon, H. T. (2015). Endophilin marks and controls a clathrin-independent endocytic pathway. *Nature* **517**, 460-465.

Bougnères, L., Helft, J., Tiwari, S., Vargas, P., Chang, B. H.-J., Chan, L., Campisi, L., Lauvau, G., Hugues, S., Kumar, P. et al. (2009). A role for lipid bodies in the cross-presentation of phagocytosed antigens by MHC class I in dendritic cells. *Immunity* **31**, 232-244.

Bucci, C., Thomsen, P., Nicoziani, P., McCarthy, J. and van Deurs, B. (2000). Rab7: a key to lysosome biogenesis. *Mol. Biol. Cell* **11**, 467-480.

Burgdorf, S., Kautz, A., Bohnert, V., Knolle, P. A. and Kurts, C. (2007). Distinct pathways of antigen uptake and intracellular routing in CD4 and CD8 T cell activation. *Science* **316**, 612-616.

Burgdorf, S., Schölz, C., Kautz, A., Tampé, R. and Kurts, C. (2008). Spatial and mechanistic separation of cross-presentation and endogenous antigen presentation. *Nat. Immunol.* **9**, 558-566.

Cebrian, I., Visentin, G., Blanchard, N., Jouve, M., Bobard, A., Moita, C., Enninga, J., Moita, L. F., Amigorena, S. and Savina, A. (2011). Sec22b regulates phagosomal maturation and antigen crosspresentation by dendritic cells. *Cell* **147**, 1355-1368.

Ceresa, B. P. and Bahr, S. J. (2006). Rab7 activity affects epidermal growth factor: epidermal growth factor receptor degradation by regulating endocytic trafficking from the late endosome. *J. Biol. Chem.* **281**, 1099-1106.

Cruzeiro-Hansson, L. and Mouritsen, O. G. (1988). Passive ion permeability of lipid membranes modelled via lipid-domain interfacial area. *Biochim. Biophys. Acta* **944**, 63-72.

de Virgilio, M., Lombardi, A., Caliandro, R. and Fabbrini, M. S. (2010). Ribosome-inactivating proteins: from plant defense to tumor attack. *Toxins* **2**, 2699-2737.

Del Nery, E., Miserey-Lenkei, S., Falguières, T., Nizak, C., Johannes, L., Perez, F. and Goud, B. (2006). Rab6A and Rab6A′ GTPases play non-overlapping roles in membrane trafficking. *Traffic* **7**, 394-407.

Donta, S. T., Tomicic, T. K. and Donohue-Rolfe, A. (1995). Inhibition of Shiga-like toxins by brefeldin A. *J. Infect. Dis.* **171**, 721-754.

Dyve Lingelem, A. B., Bergan, J. and Sandvig, K. (2012). Inhibitors of intravesicular acidification protect against Shiga toxin in a pH-independent manner. *Traffic* **13**, 443-454.

Falguières, T. and Johannes, L. (2006). Shiga toxin B-subunit binds to the chaperone BiP and the nucleolar protein B23. *Biol. Cell* **98**, 125-134.

Falguieres, T., Mallard, F., Baron, C., Hanau, D., Lingwood, C., Goud, B., Salamero, J. and Johannes, L. (2001). Targeting of Shiga toxin B-subunit to retrograde transport route in association with detergent-resistant membranes. *Mol. Biol. Cell* **12**, 2453-2468.

Gentschev, I., Dietrich, G., Spreng, S., Kolb-Mäurer, A., Daniels, J., Hess, J., Kaufmann, S. H. E. and Goebel, W. (2000). Delivery of protein antigens and DNA by virulence-attenuated strains of Salmonella typhimurium and Listeria monocytogenes. *J. Biotechnol.* **83**, 19-26.

Girard, E., Chmiest, D., Fournier, N., Johannes, L., Paul, J.-L., Vedie, B. and Lamaze, C. (2014). Rab7 is functionally required for selective cargo sorting at the early endosome. *Traffic* **15**, 309-326.

Godard, B., Gazagne, A., Gey, A., Baptiste, M., Vingert, B., Pegaz-Fiornet, B., Strompf, L., Fridman, W. H., Glotz, D. and Tartour, E. (2004). Optimization of an elispot assay to detect cytomegalovirus-specific CD8+ T lymphocytes. *Hum. Immunol.* **65**, 1307-1318.

Guermonprez, P., Saveanu, L., Kleijmeer, M., Davoust, J., Van Endert, P. and Amigorena, S. (2003). ER–phagosome fusion defines an MHC class I cross-presentation compartment in dendritic cells. *Nature* **425**, 397-402.

Haicheur, N., Bismuth, E., Bosset, S., Adotevi, O., Warnier, G., Lacabanne, V., Regnault, A., Desaymard, C., Amigorena, S., Ricciardi-Castagnoli, P. et al. (2000). The B subunit of Shiga toxin fused to a tumor antigen elicits CTL and targets dendritic cells to allow MHC class I-restricted presentation of peptides derived from exogenous antigens. *J. Immunol.* **165**, 3301-3308.

Haicheur, N., Benchetrit, F., Amessou, M., Leclerc, C., Falguières, T., Fayolle, C., Bismuth, E., Fridman, W. H., Johannes, L. and Tartour, E. (2003). The B subunit of Shiga toxin coupled to full-size antigenic protein elicits humoral and cell-mediated immune responses associated with a Th1-dominant polarization. *Int. Immunol.* **15**, 1161-1171.

Jancic, C., Savina, A., Wasmeier, C., Tolmachova, T., El-Benna, J., Dang, P. M.-C., Pascolo, S., Gougerot-Pocidalo, M.-A., Raposo, G., Seabra, M. C. et al. (2007). Rab27a regulates phagosomal pH and NADPH oxidase recruitment to dendritic cell phagosomes. *Nat. Cell Biol.* **9**, 367-378.

Johannes, L., Parton, R. G., Bassereau, P. and Mayor, S. (2015). Building endocytic pits without clathrin. *Nat. Rev. Mol. Cell Biol.* **16**, 311–321.

Kasturi, S. P. and Pulendran, B. (2008). Cross-presentation: avoiding trafficking chaos? *Nat. Immunol.* **9**, 461-463.

Keller, C., Mellouk, N., Danckaert, A., Simeone, R., Brosch, R., Enninga, J. and Bobard, A. (2013). Single cell measurements of vacuolar rupture caused by intracellular pathogens. *J. Vis. Exp.*, **76**, e50116.

Lee, R.-S., Tartour, E., Van der Bruggen, P., Vantomme, V., Joyeux, I., Goud, B., Fridman, W. H. and Johannes, L. (1998). Major histocompatibility complex class I presentation of exogenous soluble tumor antigen fused to the B-fragment of Shiga toxin. *Eur. J. Immunol.* **28**, 2726-2737.

Lewis, M. J., Rayner, J. C. and Pelham, H. R. B. (1997). A novel SNARE complex implicated in vesicle fusion with the endoplasmic reticulum. *EMBO J.* **16**, 3017-3024.

Mallard, F. and Johannes, L. (2003). Shiga toxin B-subunit as a tool to study retrograde transport. *Methods Mol. Med.* **73**, 209-220.

Mallard, F., Antony, C., Tenza, D., Salamero, J., Goud, B. and Johannes, L. (1998). Direct pathway from early/recycling endosomes to the Golgi apparatus revealed through the study of shiga toxin B-fragment transport. *J. Cell Biol.* **143**, 973-990.

Mallard, F., Tang, B. L., Galli, T., Tenza, D., Saint-Pol, A., Yue, X., Antony, C., Hong, W., Goud, B. and Johannes, L. (2002). Early/recycling endosomes-to-TGN transport involves two SNARE complexes and a Rab6 isoform. *J. Cell Biol.* **156**, 653-664.

Mohrmann, K. and van der Sluij, P. (1999). Regulation of membrane transport through the endocytic pathway by rabGTPases. *Mol. Membr. Biol.* **16**, 81-87.

Noel, R., Gupta, N., Pons, V., Goudet, A., Garcia-Castillo, M. D., Michau, A., Martinez, J., Buisson, D.-A., Johannes, L., Gillet, D. et al. (2013). N-methyldihydroquinazolinone derivatives of Retro-2 with enhanced efficacy against Shiga toxin. *J. Med. Chem.* **56**, 3404-3413.

Pere, H., Montier, Y., Bayry, J., Quintin-Colonna, F., Merillon, N., Dransart, E., Badoual, C., Gey, A., Ravel, P., Marcheteau, E. et al. (2011). A CCR4 antagonist combined with vaccines induces antigen-specific CD8+ T cells and tumor immunity against self antigens. *Blood* **118**, 4853-4862.

Ploegh, H. L. (2007). A lipid-based model for the creation of an escape hatch from the endoplasmic reticulum. *Nature* **448**, 435-438.

Polito, L., Bortolotti, M., Pedrazzi, M. and Bolognesi, A. (2011). Immunotoxins and other conjugates containing saporin-s6 for cancer therapy. *Toxins* **3**, 697-720.

Ramegowda, B. and Tesh, V. L. (1996). Differentiation-associated toxin receptor modulation, cytokine production, and sensitivity to Shiga-like toxins in human monocytes and monocytic cell lines. *Infect. Immun.* **64**, 1173-1180.

Ray, K., Bobard, A., Danckaert, A., Paz-Haftel, I., Clair, C., Ehsani, S., Tang, C., Sansonetti, P., Van Nhieu, G. T. and Enninga, J. (2010). Tracking the dynamic interplay between bacterial and host factors during pathogen-induced vacuole rupture in real time. *Cell. Microbiol.* **12**, 545-556.

Renard, H.-F., Simunovic, M., Lemière, J., Boucrot, E., Garcia-Castillo, M. D., Arumugam, S., Chambon, V., Lamaze, C., Wunder, C., Kenworthy, A. K. et al. (2015). Endophilin-A2 functions in membrane scission in clathrin-independent endocytosis. *Nature* **517**, 493-496.

Rojas, R., van Vlijmen, T., Mardones, G. A., Prabhu, Y., Rojas, A. L., Mohammed, S., Heck, A. J. R., Raposo, G., van der Sluijs, P. and Bonifacino, J. S. (2008). Regulation of retromer recruitment to endosomes by sequential action of Rab5 and Rab7. *J. Cell Biol.* **183**, 513-526.

Sandoval, F., Terme, M., Nizard, M., Badoual, C., Bureau, M.-F., Freyburger, L., Clement, O., Marcheteau, E., Gey, A., Fraisse, G. et al. (2013). Mucosal imprinting of vaccine-induced CD8+ T cells is crucial to inhibit the growth of mucosal tumors. *Sci. Transl. Med.* **5**, 172ra20.

Santanché, S., Bellelli, A. and Brunori, M. (1997). The unusual stability of saporin, a candidate for the synthesis of immunotoxins. *Biochem. Biophys. Res. Commun* **234**, 129-132.

Savina, A., Jancic, C., Hugues, S., Guermonprez, P., Vargas, P., Moura, I. C., Lennon-Duménil, A.-M., Seabra, M. C., Raposo, G. and Amigorena, S. (2006).

NOX2 controls phagosomal pH to regulate antigen processing during crosspresentation by dendritic cells. *Cell* **126**, 205-218.

Savina, A., Peres, A., Cebrian, I., Carmo, N., Moita, C., Hacohen, N., Moita, L. F. and Amigorena, S. (2009). The small GTPase Rac2 controls phagosomal alkalinization and antigen crosspresentation selectively in CD8+ dendritic cells. *Immunity* **30**, 544-555.

Semerdjieva, S., Shortt, B., Maxwell, E., Singh, S., Fonarev, P., Hansen, J., Schiavo, G., Grant, B. D. and Smythe, E. (2008). Coordinated regulation of AP2 uncoating from clathrin-coated vesicles by rab5 and hRME-6. *J. Cell Biol.* **183**, 499-511.

Shin, H. W., Hayashi, M., Christoforidis, S., Lacas-Gervais, S., Hoepfner, S., Wenk, M. R., Modregger, J., Uttenweiler-Joseph, S., Wilm, M., Nystuen, A. et al. (2005). An enzymatic cascade of Rab5 effectors regulates phosphoinositide turnover in the endocytic pathway. *J. Cell Biol.* **170**, 607-618.

Simeone, R., Bobard, A., Lippmann, J., Bitter, W., Majlessi, L., Brosch, R. and Enninga, J. (2012). Phagosomal rupture by Mycobacterium tuberculosis results in toxicity and host cell death. *PLoS Pathog.* **8**, e1002507.

Smith, D. C., Lord, J. M., Roberts, L. M., Tartour, E. and Johannes, L. (2002). 1st class ticket to class I: protein toxins as pathfinders for antigen presentation. *Traffic* **3**, 697-704.

Smith, D. C., Marsden, C. J., Lord, J. M. and Roberts, L. M. (2003). Expression, Purification and Characterization of Ricin vectors used for exogenous antigen delivery into the MHC Class I presentation pathway. *Biol. Proced. Online* **5**, 13-19.

Spooner, R. A. and Lord, J. M. (2012). How ricin and Shiga toxin reach the cytosol of target cells: retrotranslocation from the endoplasmic reticulum. *Curr. Top. Microbiol. Immunol.* **357**, 19-40.

Stechmann, B., Bai, S.-K., Gobbo, E., Lopez, R., Merer, G., Pinchard, S., Panigai, L., Tenza, D., Raposo, G., Beaumelle, B. et al. (2010). Inhibition of retrograde transport protects mice from lethal ricin challenge. *Cell* **141**, 231-242.

Tam, P. J. and Lingwood, C. A. (2007). Membrane cytosolic translocation of verotoxin A1 subunit in target cells. *Microbiology* **153**, 2700-2710.

Tarr, P. I., Gordon, C. A. and Chandler, W. L. (2005). Shiga-toxin-producing Escherichia coli and haemolytic uraemic syndrome. *Lancet* **365**, 1073-1086.

Uchide, N. and Toyoda, H. (2007). A new simple multi-well plate-based assay for monocyte differentiation using human monocytic leukemia THP-1 cells. *J. Immunol. Methods* **328**, 215-219.

Vanlandingham, P. A. and Ceresa, B. P. (2009). Rab7 regulates late endocytic trafficking downstream of multivesicular body biogenesis and cargo sequestration. *J. Biol. Chem.* **284**, 12110-12124.

Vingert, B., Adotevi, O., Patin, D., Jung, S., Shrikant, P., Freyburger, L., Eppolito, C., Sapoznikov, A., Amessou, M., Quintin-Colonna, F. et al. (2006). The Shiga toxin B-subunit targets antigen in vivo to dendritic cells and elicits anti-tumor immunity. *Eur. J. Immunol.* **36**, 1124-1135.

Wagner, C. S., Grotzke, J. E. and Cresswell, P. (2012). Intracellular events regulating cross-presentation. *Front. Immunol.* **3**, 138.

SUPPLEMENTARY MATERIAL

Supplementary Figure 1: Analysis of STxB-saporin conjugates.

(A) SDS-PAGE was performed on a Tris-Tricine gel, and proteins stained with Coomasie Blue. Lane 1, non-cleavable *STxB-saporin*; Lane 2, cleavable *STxB-ss-saporin*; Lane 3, STxB-Cys; Lane 4 and Lane 6, cleavable *STxB-ss-saporin* +DTT; Lane 5, non-cleavable *STxB-saporin* +DTT; Lane 7, unconjugated saporin. **(B)** N-glycosidase activity of unconjugated saporin versus *STxB-ss-saporin*. **(C)** N-glycosidase activity of non-cleavable *STxB-saporin* versus cleavable *STxB-ss-saporin*. Percent depurination was calculated by relating the aniline fragment (arrow head) to the 5.8s rRNA. A non-aniline, toxin-treated control is shown.

Supplementary Figure 2: Retrograde transport inhibition of *STxB-ss-saporin* in HeLa cells.

(A) HeLa cells stably expressing GFP-tagged endoA2 incubated with 0.2 μM STxB-Cy3 or 0.1 μM STxB-ss-saporin and analyzed by total internal reflection microscopy. Scale bar: 5 μm. **(B)** 50 nM STxB-Cy3 and 50 nM Cy3-coupled STxB-ss-saporin were bound to HeLa cells on ice, which were subsequently incubated for 5 minutes at 37°C. Labelings were then analyzed by confocal microscopy. Note the substantial colocalization between both makers. Pearson's correlation coefficient is reported. Scale bar: 10 μm. **(C)** 0.5 μg/ml *STxB-ss-saporin* was incubated for 45 minutes at 37°C with HeLa cells in the absence or presence of 25 μM Retro-2. After washing, immunofluoresence was perfomed using anti-STxB (red) and anti-giantin (green) antibodies, and cells were analyzed by confocal microscopy. Scale bars: 10 μm. **(D)** Immunofluoresence experiments were also perfomed using anti-STxB (red) and goat anti-saporin (green) antibodies in control or Retro-2 treated cells, as described in **(C)**. Scale bars: 10 μm.

Supplementary Figure 3: Effect of temperature and endosomal acidification on *STxB-ss-saporin* cytotoxicity.

(A) Representative intoxication assay after a 4 hour exposure to STx-1 or *STxB-ss-saporin* in control conditions (black curves) or at 19.5°C (red curves). **(B)** Similarly, intoxication assays were perfomed after bafilomycin A1 treatment. A representative experiment is shown.
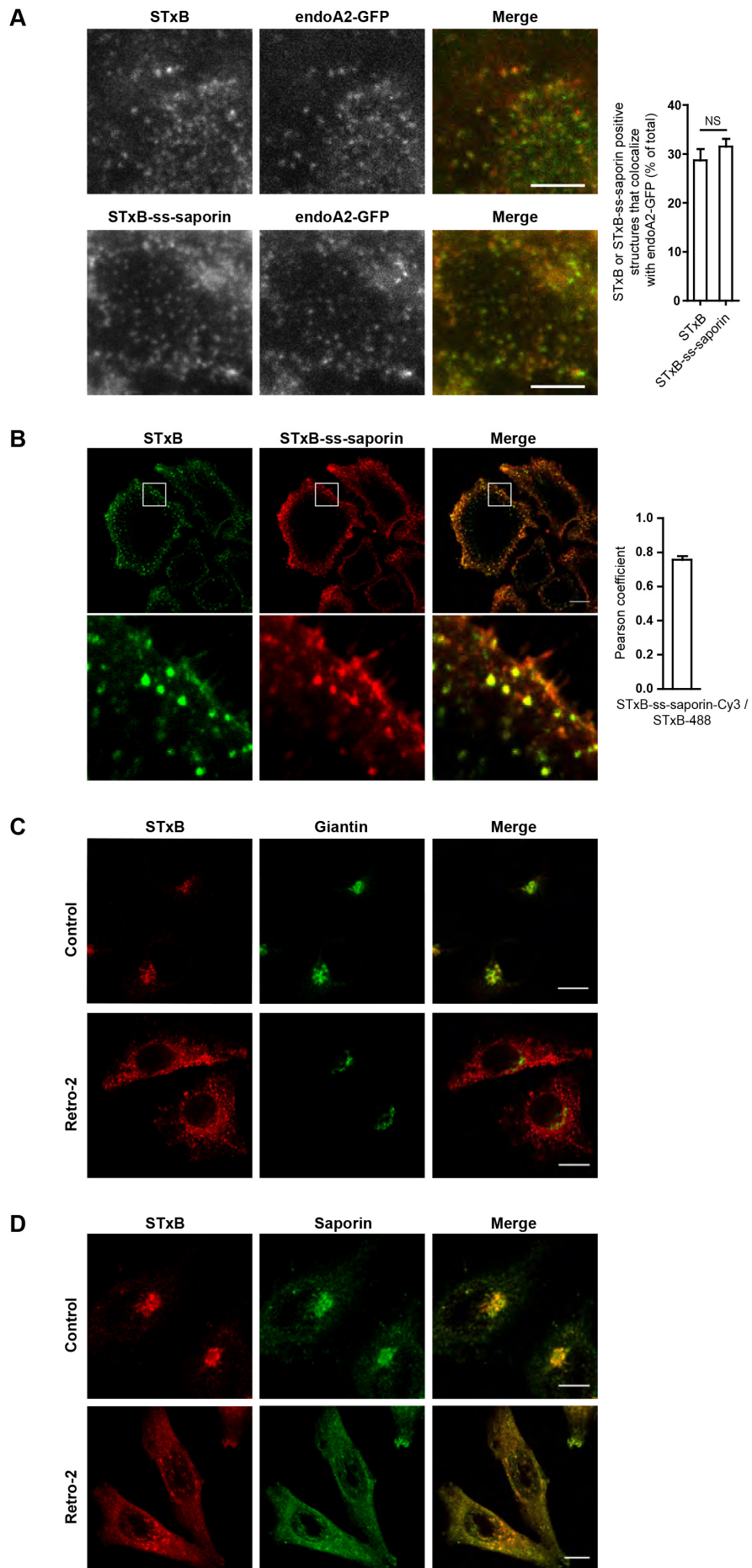
1   **Supplementary Figure 4: Western Blot analysis of Sec22B, Rab6a', Rab5, or Rab7**

2   **depletion.**

3   Western blot analysis of siRNA-mediated depletion of **(A)** Sec22B, **(B)** Rab6a', **(C)** Rab5, or **(D)**

4   Rab7 versus control (scrambled) siRNA using antibodies against each of these proteins and CHC
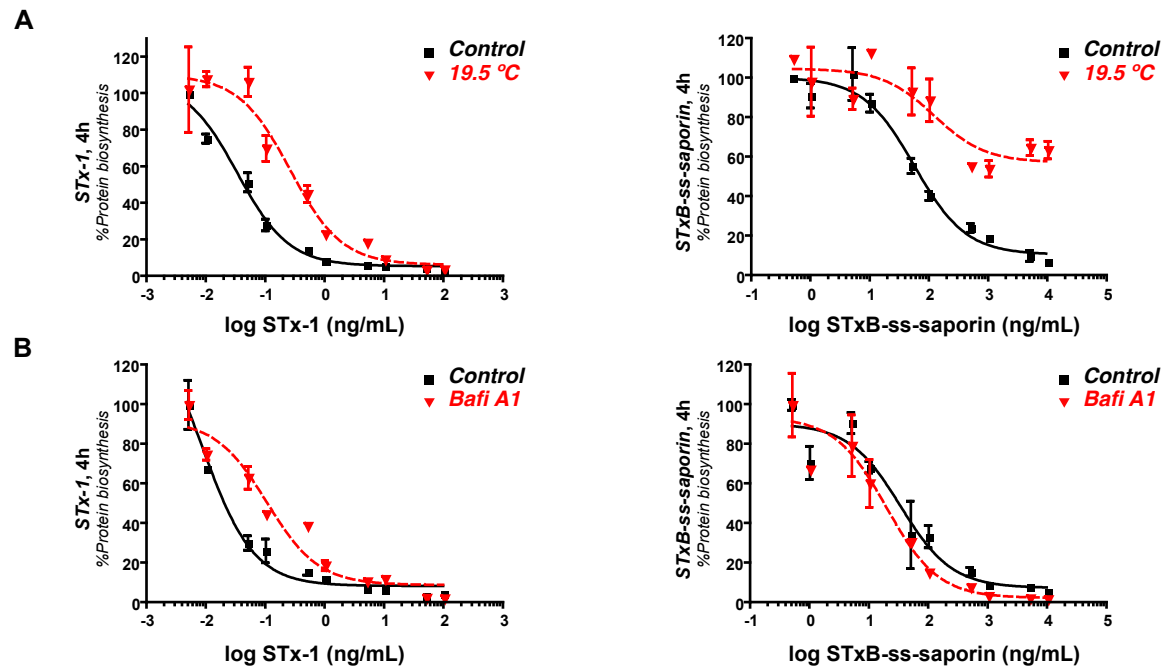
5   (clathrin heavy chain) as a loading control.

6

7

8

Supplementary Figure 1. Garcia-Castillo *et al*.

A

B

C
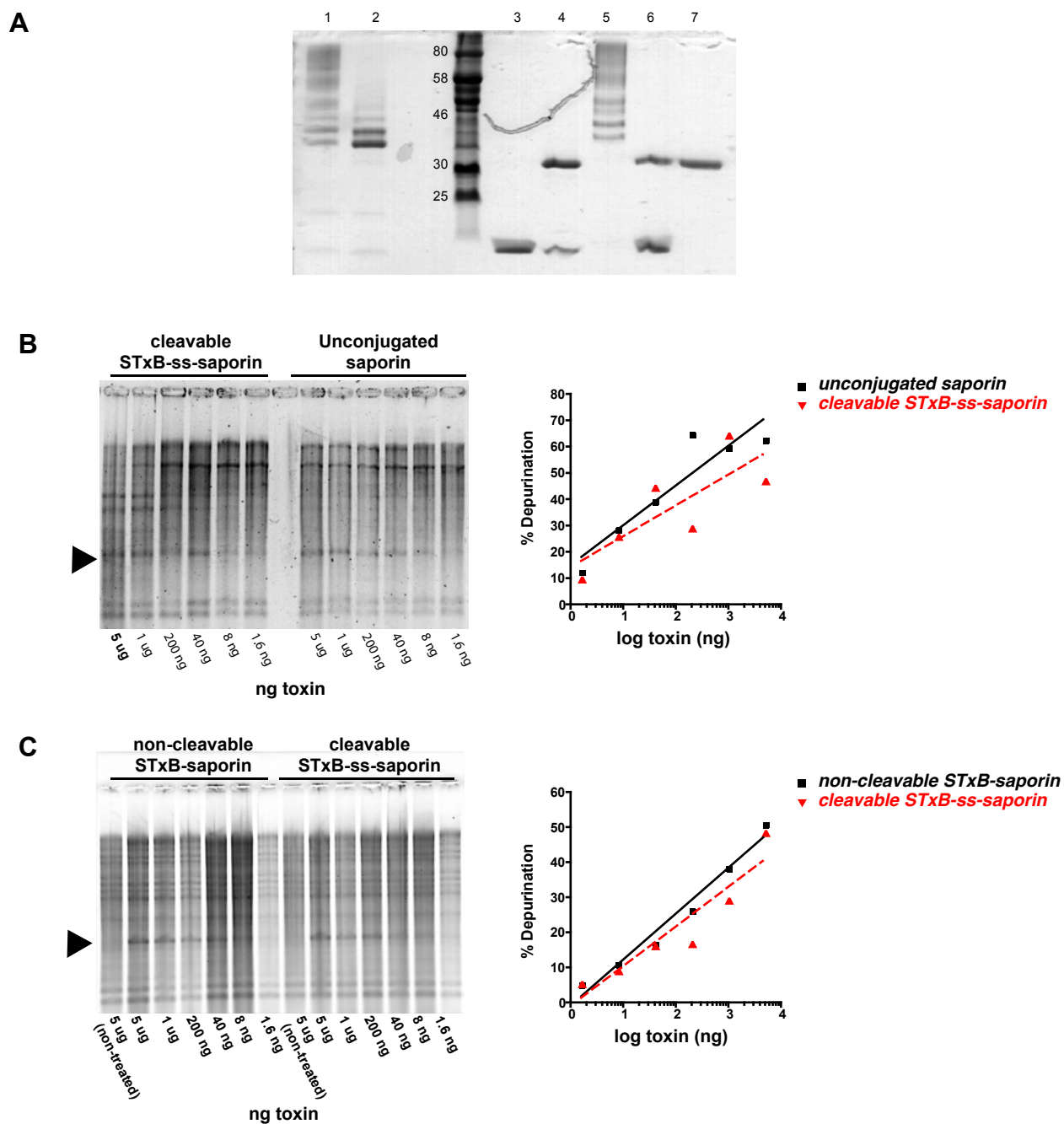
Supplementary Figure 2. Garcia-Castillo *et al*.

Supplementary Figure 3. Garcia-Castillo *et al.*

A

B

Supplementary Figure 4. Garcia-Castillo *et al.*

A CT   Sec22B siRNA

Sec22B

CHC

B CT   Rab6 siRNA

Rab 6

CHC

C CT   Rab5 siRNA

Rab-5

CHC

D CT   Rab7 siRNA

Rab-7

CHC